A revamped rat reference genome improves the discovery of genetic diversity in laboratory rats*

Tristan V de Jong, [1†] Yanchao Pan, [2†] Pasi Rastas, [3] Daniel Munro, [4,5] Monika Tutaj, [6,7] Huda Akil, [8] Chris Benner, [9] Denghui Chen, [4] Apurva S Chitre, [4] William Chow, [10] Vincenza Colonna, [11,12] Clifton L Dalgard, [13] Wendy M Demos, [6,7] Peter A Doris, [14] Erik Garrison, [12] Aron M Geurts, [6] Hakan M Gunturkun, [1] Victor Guryev, [15] Thibaut Hourlier, [16] Kerstin Howe, [10] Jun Huang, [1] Ted Kalbfleisch, [17] Panjun Kim, [12] Ling Li, [12,18] Spencer Mahaffey, [19] Fergal J Martin, [16] Pejman Mohammadi, [20,21] Ayse Bilge Ozel, [2] Oksana Polesskaya, [4] Michal Pravenec, [22] Pjotr Prins, [12] Jonathan Sebat, [4] Jennifer R Smith, [6,7] Leah C Solberg Woods, [23] Boris Tabakoff, [19] Alan Tracey, [10] Marcela Uliano-Silva, [10] Flavia Villani, [12] Hongyang Wang, [24] Burt M Sharp, [12] Francesca Telese, [4] Zhihua Jiang, [24] Laura Saba, [19] Xusheng Wang, [12,18] Terence D Murphy, [25] Abraham A Palmer, [4,26] Anne E Kwitek, [6,7] Melinda R Dwinell, [6,7] Robert W Williams, [12] Jun Z Li, [2‡] Hao Chen [1‡]

1 Department of Pharmacology, Addiction Science, and Toxicology, University of Tennessee Health Science Center, Memphis, TN, USA
2 Department of Human Genetics, University of Michigan, Ann Arbor, MI, USA
3 Institute of Biotechnology, University of Helsinki, Helsinki, Finland
4 Department of Psychiatry, University of California San Diego, San Diego, CA, USA
5 Department of Integrative Structural and Computational Biology, Scripps Research, San Diego, CA, USA
6 Department of Physiology, Medical College of Wisconsin, Milwaukee, WI, USA
7 Rat Genome Database, Medical College of Wisconsin, Milwaukee, WI, USA
8 Michigan Neuroscience Institute, University of Michigan, Ann Arbor, MI, USA
9 Department of Medicine, University of California San Diego, San Diego, CA, USA
10 Tree of Life, Wellcome Sanger Institute, Cambridge, UK
11 Institute of Genetics and Biophysics, National Research Council, Naples, Italy
12 Department of Genetics, Genomics and Informatics, University of Tennessee Health Science Center, Memphis, TN, USA
13 Department of Anatomy, Physiology & Genetics; The American Genome Center, Uniformed Services University of the Health Sciences, Washington DC, USA
14 The Brown Foundation Institute of Molecular Medicine, Center For Human Genetics, University of Texas Health Science Center, Houston, TX, USA
15 Genome Structure and Ageing, University of Groningen, UMC Groningen, The Netherlands
16 European Molecular Biology Laboratory, European Bioinformatics Institute, Wellcome Genome Campus in Hinxton, Cambridgeshire, UK
17 Gluck Equine Research Center, Department of Veterinary Science, University of Kentucky, Louisville, KY, USA
18 Center for Proteomics and Metabolomics, St. Jude Children's Research Hospital, Memphis, TN, USA
19 Department of Pharmaceutical Sciences, Skaggs School of Pharmacy and Pharmaceutical Sciences, University of Colorado Anschutz Medical Campus, Aurora, CO, USA
20 Center for Immunity and Immunotherapies, Seattle Children's Research Institute, Seattle, WA, USA
21 Department of Pediatrics, University of Washington School of Medicine, Seattle, WA, USA
22 Institute of Physiology, Czech Academy of Sciences, Prague, Czechia
23 Department of Internal Medicine, Section on Molecular Medicine, Wake Forest University School of Medicine, Winston-Salem, NC, USA
24 Department of Animal Sciences, Washington State University, Pullman, WA, USA
25 National Center for Biotechnology Information, National Library of Medicine, National Institutes of Health, Bethesda, MD, USA
26 Institute for Genomic Medicine, University of California San Diego, La Jolla, CA, USA

---

* Dedicated to the memory of Dr. Mary Shimoyama.

† These authors made equal contributions to the work.

‡ Corresponding authors. E-mails: junzli@med.umich.edu hchen@uthsc.edu

Summary

The seventh iteration of the reference genome assembly for *Rattus norvegicus*—mRatBN7.2—corrects numerous misplaced segments and reduces base-level errors by approximately 9-fold and increases contiguity by 290-fold compared to its predecessor. Gene annotations are now more complete, significantly improving the mapping precision of genomic, transcriptomic, and proteomics data sets. We jointly analyzed 163 short-read whole genome sequencing datasets representing 120 laboratory rat strains and substrains using mRatBN7.2. We defined ~20.0 million sequence variations, of which 18.7 thousand are predicted to potentially impact the function of 6,677 genes. We also generated a new rat genetic map from 1,893 heterogeneous stock rats and annotated transcription start sites and alternative polyadenylation sites. The mRatBN7.2 assembly, along with the extensive analysis of genomic variations among rat strains, enhances our understanding of the rat genome, providing researchers with an expanded resource for studies involving rats.

Keywords

Rat, Reference Genome, mRatBN7.2, Rnor_6.0, Hybrid Rat Diversity Panel, Heterogeneous Stock, Genetic Map, Phylogenetic Tree, Inbred Strains, Recombinant Inbred

Introduction

Rattus norvegicus was among the first mammalian species used for scientific research. The earliest studies using brown rats appeared in the early 1800s. [1,2] The Wistar rats were bred for scientific research in 1906, and is the ancestor of many laboratory strains. [3] Rats have been used as models in many fields of study related to human disease due to their body sizes large enough for easy phenotyping and showing complex physiological and behavioral patterns. [4]

Over 4,000 inbred, outbred, congenic, mutant, and transgenic strains have been created and are documented in the Rat Genome Database (RGD). [5] Approximately 500 are available from the Rat Resource and Research Center. [6] Several genetic reference populations are also available, including the HXB/BXH [7] and FXLE/LEXF [8] recombinant inbred (RI) families. Both families, together with 30 diverse classical inbred strains, [9] are now part of the Hybrid Rat Diversity Panel (HRDP), which can be used to quickly generate any of over 10,000 isogenic and replicable F_1 hybrids—all of which are now essentially sequenced. The outbred N/NIH heterogeneous stocks (HS) rats, derived from eight inbred strains, [10] have been increasingly used for fine mapping of physiological and behavioral traits. [11–15] To date, RGD has annotated nearly 2,400 rat quantitative trait loci (QTL), [16] mapped using F2 crosses, RI families, and HS rats.

The *Rattus norvegicus* was sequenced shortly after the genomes of *Homo sapiens* and *Mus musculus*. [17] The inbred Brown Norway (BN/SsNHsdMcwi) strain, derived by many generations of sibling matings of stock originally from a pen-bred colony of wild rats, [3] was used to generate the reference. Several updates were released over the following decade. [18–20] Since 2014, most rat genomic and genetic research used the incomplete and problematic Rnor_6.0 assembly. [21] [22] mRatBN7.2 was created in 2020 by the Darwin Tree of Life/Vertebrate Genome Project (VGP) as the new genome assembly of the BN/NHsdMcwi rat. [23] The genome reference consortium (GRC, https://www.ncbi.nih.gov/grc/rat) has adopted mRatBN7.2 as the official rat reference genome.

Here we report extensive analyses of the improvements in mRatBN7.2 compared to Rnor_6.0. To assist the rat research community in transitioning to mRatBN7.2, we conducted a broad analysis of a whole-genome sequencing (WGS) dataset of 163 samples from 120 inbred rat strains and substrains. Joint variant calling led to the discovery of 19,987,273 high quality variants from 15,804,627 sites. Additional resources created during our analysis included a rat genetic map with 150,835 markers, a comprehensive phylogenetic tree for the 120 strains, and extensive annotation of identified genes, including their transcription start sites and alternative polyadenylation

sites. This new assembly and its associated resources create a more solid platform for research on the many dimensions of physiology, behavior, and pathobiology of rats, and for more reliable and meaningful translation of findings to human populations.

Results

High structural and base-level accuracy of mRatBN7.2

mRatBN7.2 [23] was generated as part of the Darwin Tree of Life/Vertebrate Genome Project. All sequencing data were generated from a male Brown Norway (BN) rat from the Medical College of Wisconsin (BN/NHsdMcwi, generation F61). The assembly is based on integrating data across multiple technologies, including long-read sequencing (PacBio CLR), 10X linked-read sequencing, BioNano DLS optical map, and Arima HiC. After automated assembly, manual curation corrected most of the apparent discrepancies among data types. [24] While mRatBN7.2 contains an alternative pseudo-haplotype (GCA_015244455.1), we focused our analysis on the primary assembly (GCF_015227675.2). In November 2020, mRatBN7.2 was accepted by the Genome Reference Consortium (GRC) as the new rat reference genome, and the Rat Genome Database (RGD) joined the GRC to oversee its curation.

Over the last six iterations of the rat reference, genome continuity has improved incrementally (Table S1). Contig N50, one measure of assembly quality, has been ~30 Kb between rn1 to rn5. Rnor_6.0 was the first assembly to include some long-read PacBio data and improved contig N50 to 100.5 Kb. mRatBN7.2 further improved N50 to 29.2 Mb (Figure S1). Although this measure of contiguity lags slightly behind the mouse reference genome (contig N50=59 Mb in GRCm39, released in 2020), and far behind the first Telomere-to-Telomere human genome (CHM13) (Table 1), it still marks a significant improvement (~290 times higher) over Rnor_6.0 (Figure S2). In another measure, the number of contigs in mRatBN7.2 was reduced by 100-fold compared to Rnor_6.0, and is approaching the quality of GRCh38 for humans and GRCm39 for mice (Table 1).

Although aligning Rnor_6.0 with mRatBN7.2 showed a high level of structural agreement (Figure 1A, Figure S3), we identified 36,500 discordant segments between these two assemblies that are longer than 50 bp (Figure S4). To evaluate these differences, we generated a genetic map (Table S2) using data from 378 families of 1,893 HS rats based on the recombination frequency between 151,380 markers. [15] Comparing the order of the markers and their location on the reference confirmed that the order and orientation of genomic segment are much more accurate in mRatBN7.2. For example, there is a 17.2 Mb inverted segment at proximal Chr 6 between Rnor_6.0

and mRatBN7.2 (Figure 1B). It remains inverted when the genetic distance is plotted with marker location on Rnor_6.0 (Figure 1C), but is resolved when using marker locations on mRatBN7.2 (Figure 1D), as was also true for several other regions (e.g. Figure 1E-G for Chr 19, and Figure S5 and S6 for all autosomes). These data indicate that most of the segment-wise differences between the two assemblies are due to errors in Rnor_6.0.

We mapped linked-read WGS data for 36 samples from the HXB/BXH family of strains, against both Rnor_6.0 and mRatBN7.2. These included four samples of the reference strain (BN/NHsdMcwi), two samples from the two parental strains—SHR/OlaIpcv and BN-Lx/Cub—and all 30 extent HXB/BXH progeny strains. The mean read depth of the entire HXB dataset, including all parentals, is 105.5X (range 23.4–184.5, Table S9). From mRatBN7.2 to Rnor_6.0, the fraction of reads mapped to the reference increased by 1–3% (Figure 2A), and regions of the genome with no coverage decreased by ~2% (Figure 2B). Genetic variants (SNPs and indels) were identified using *deepvariant* [25] and jointly called for the 36 samples using *GLnexus.* [26] After quality filtering (qual ≥ 30) of HXB sequence we identified ~11.8 million variants (8,286,401SNPs and 3,527,568 indels) in mRatBN7.2. Corresponding numbers for Rnor_6.0 are 5,088,144 SNPs and 1,615,870 indels (Figure 2C, 2D). Surprisingly, variants shared by all 36 samples—either homozygous in all samples or heterozygous in all samples—were more abundant when aligned to Rnor_6.0 (1,310,902) than to mRatBN7.2 (143,254) (Figure 2E, 2F). Because we included sequence data from 4 BN/NHsdMcwi rats, *including those used for both Rnor_6.0 and mRatBN7.2,* the most parsimonious explanation is that these shared variants are due to the wrong nucleotide sequence being recorded as the reference allele in the references. Therefore, mRatBN7.2 also reduced base-level errors by 9.2-fold compared to Rnor_6.0. A more detailed analysis of segment-level errors in mRatBN7.2 is provided below.

Improved gene model annotations in mRatBN7.2

mRatBN7.2-based gene annotations were released in RefSeq 108 and Ensembl 105 (supplemental methods). For both RefSeq and Ensembl, the updated gene models were derived from multiple data sources, including past transcriptomic datasets and newly revised multi-species sequence alignments.

We compared the Rnor6.0 and mRatBN7.2 annotation sets in RefSeq using BUSCO v4.1.4, [27] focusing on the glires_odb10 dataset of 13,798 genes that are expected to occur in single copy in rodents. Instead of generating a *de novo* annotation with BUSCO using the Augustus or MetaEuk gene predictors, we used proteins from the new annotations, picking one longest protein per gene for analysis. BUSCO reported 98.7% of the glires_odb10 genes as complete in RefSeq 108 [Single-copy (S):97.2%,

Duplicated (D):1.5, Fragmented (F):0.4%, Missing (M):0.9%]. In comparison, analysis of Rnor_6.0 with NCBI's annotation pipeline using the same code and evidence sets showed a slightly higher fraction of fragmented and missing genes, and more than double the rate of duplicated genes (S:94.4%, D:3.3%, F:0.9%, M:1.4%). The Ensembl annotation was evaluated using BUSCO version 5.3.2 with the lineage dataset "glires_odb10/2021-02-19". The "complete and single-copy BUSCO" score improved from 93.6% to 95.3%, and the overall score improved from 96.5% in Rnor_6.0 to 97.0% in mRatBN7.2. Both annotation sets demonstrate that mRatBN7.2 is a better foundation for gene annotation, with improved representation of protein-coding genes.

RefSeq (release 108) annotated 42,167 genes, each associated with a unique NCBI GeneID. These included 22,228 protein-coding genes, 7,888 lncRNA, 1,288 snoRNA, 1,026 snRNA, and 7,972 pseudogenes. Ensembl (release 107) annotation contained 30,559 genes identified with unique "ENSRNOG" stable IDs. These included 23,096 protein-coding genes, 2,488 lncRNA, 1,706 snoRNA, 1,512 snRNA, and 762 pseudogenes. Although the two transcriptomes have similar numbers of protein-coding genes, RefSeq annotates many more lncRNA (more than 3X) and pseudogenes (almost 10X), and only RefSeq annotates tRNA.

Comparing individual genes across the two annotation sets, Ensembl BioMart reported 23,074 Ensembl genes with an NCBI GeneID, and NCBI Gene reported 24,115 RefSeq genes with an Ensembl ID (Table S3). We note that 2,319 protein-coding genes were annotated with different names (Table S4). While many of these were caused by the lack of formal gene names in one of the sources, some of them were annotated with distinct names. For example, some widely studied genes, such as *Bcl2*, *Cd4*, *Adrb2*, etc., were not annotated with GeneID in Ensembl BioMart. We found that 18,722 gene symbols were annotated in both RefSeq and Ensembl. Among the 22,247 gene symbols found only in RefSeq, 20,185 were genes without formal names. Further, RefSeq contained a total of 100,958 transcripts, with an average of 2.9 (range: 1–51) transcripts per gene. Ensembl had 54,991 transcripts, with an average of 1.8 (range: 1–10) transcripts per gene (Figure S7).

mRatBN7.2 improved the mapping of WGS data

In addition to short read WGS data (see above), we also compared mapping results of long-read datasets. Unmapped read numbers declined from 298,422 in Rnor_6.0 to 260,947 in mRatBN7.2, a 12.6% reduction using a PacBio CLR dataset from an SHR rat with a total of 4,508,208 reads. Mapping of Nanopore data from one outbred HS rat (~55X coverage) showed much lower secondary alignment—from ~10 million in Rnor_6.0 to 4 million in mRatBN7.2. Similar to the linked-read data, structural variants detected in the Nanopore dataset were reduced (Figure S8) using mRatBN7.2.

We also evaluated the effect of reference genome on the identification of structural variants (SVs). We identified 19,538 unique SVs against Rnor_6.0 in the HXB dataset. In contrast, only 5,458 SVs were found using mRatBN7.2 (Table S5). Among these SVs, 5,326 deletions were found using Rnor_6.0, and only 1,045 deletions were reported using mRatBN7.2. We illustrated these findings by focusing on a small panel of eight samples (Figure S9). The sample with the greatest number of deletions (HXB21) showed a reduction from 1,017 in Rnor_6.0 to 110 in mRatBN7.2. These results corroborated the findings from the analysis of SNPs that mRatBN7.2 eliminates many errors in Rnor_6.0.

mRatBN7.2 improved the analysis of transcriptomic and proteomic data

We analyzed an RNA-seq dataset of 352 HS rat brains (see RatGTEx.org) to compare the effect of the reference genome. The fraction of reads aligned to the reference increased from 97.4% in Rnor_6.0 to 98.3% in mRatBN7.2. The average percent of reads aligned concordantly only once to the reference genome increased from 89.3 to 94.6%. The average percent of reads aligned to the Ensembl transcriptome increased from 67.7 to 74.8%. Likewise, we examined the alignment of RNA-seq data from ribosomal RNA-depleted total RNA and short RNA in the HRDP. For the total RNA (>200 bp) samples, alignment to the genome increased from 92.4% to 94.0%, while the percentage of reads aligned concordantly only once to the reference increased from 76.1% to 79.2%. For the short RNA (<200 bp; targeting transcripts 20–50 bp long), genome alignment increased from 95.0% to 96.2% and unique alignment increased from 33.2% to 35.9%. In an snRNA-seq dataset (Figure S10), the percentage of reads that mapped confidently to the reference increased from 87.4% on Rnor_6.0 to 91.4% on mRatBN7.2. In contrast, reads mapped with high quality to intergenic regions were reduced from 24.5% on Rnor_6.0 to 10.3% on mRatBN7.2.

We analyzed datasets containing information about transcript start and polyadenylation in a capped short RNA-seq (csRNA-seq) data set. The rate of unique alignment of transcriptional start sites to the reference genome increased 5% in mRatBN7.2 (Fig. S14B). In this dataset, we identified 42,420 transcription start sites when using Rnor_6.0, and 44,985 sites when using mRatBN7.2 (Table S5). We analyzed 83 whole transcriptome termini site sequencing [28] datasets using total RNA derived from rat brains, and found that 76.97% were mapped against Rnor_6.0, while 80.49% were mapped against mRatBN7.2 (Table S6). We identified 167,136 alternative polyadenylation (APA) sites using Rnor_6.0 and 73,124 APA sites using mRatBN7.2. For Rnor_6.0, only 76.26% APA sites were assigned to the genomic regions with

18,177 annotated genes (Table S6). In contrast, 81.67% APA sites were mapped to 20,102 annotated genes on mRatBN7.2 (Table S6).

We examined the impact of the upgraded reference assembly on the yield and relative numbers of expression quantitative trait locus (eQTL) using a large RNA-seq dataset for nucleus accumbens. [29] We identified associations that would be labeled as trans-eQTLs using one reference but cis-eQTL using the other, due to relocation of the SNP and/or the TSS. The expectation is that assembly errors will give rise to spurious trans-eQTLs. We found seven genes associated with one or more strong trans-eQTL SNP using Rnor_6.0 that converted to cis-eQTLs using mRatBN7.2 (Figure 3). This constitutes 5.2% (3,261 of 63,148) of the Rnor_6.0 trans-eQTL SNP-gene pairs. In contrast, only 0.01% (51 of 404,302) of the Rnor_6.0 cis-eQTL SNP-gene pairs became trans-eQTLs when using mRatBN7.2. Given the much lower probability of a distant SNP-gene pair remapping to be in close proximity than vice versa under a null model of random relocations, this demonstrates a clear improvement in the accuracy and interpretation of eQTLs when using mRatBN7.2.

To evaluate the effect of reference genome on proteome data, we analyzed a set of data from 29 HXB/BXH strains. At a peptide-identification false discovery rate (FDR) of 1%, we identified and quantified 8,002 unique proteins on Rnor_6.0, compared to 8,406 unique proteins on mRatBN7.2 (5% increase). For protein local expression quantitative trait locus (i.e., cis-pQTL), 536 were identified using Rnor_6.0 and 541 were identified using mRatBN7.2 at FDR < 5%. Distances between pQTL peaks and the corresponding gene start site tended to be shorter on mRatBN7.2 than on Rnor_6.0 (Figure 4A). Similar to eQTLs, four proteins with trans-pQTL in Rnor_6.0 were converted to cis-pQTL using mRatBN7.2. For example, RPA1 protein (Chr10:60,148,794–60,199,949 bp in mRatBN7.2) mapped as a significant trans-pQTL ($p = 1.71 \times 10^{-12}$) on Chr 4 in Rnor_6.0, but as a significant cis-pQTL using mRatBN7.2 (*p-value* = 4.12×10^{-6}) (Figure 4B). In addition, the expression of RPA1 protein displayed a high correlation between mRatBN7.2 and in Rnor_6.0 (r = 0.79; p value = 3.7×10^{-7}) (Figure 4C). Lastly, the annotations for RPA1 were different between the two references (Figure 4D).

WGS mapping data suggesting potential errors remaining in mRatBN7.2

We analyzed a whole-genome sequencing dataset of 163 inbred rats (described in Methods), containing 12 BN samples and 151 non-BN samples, which represented two RI panels and more than 30 inbred strains. After read-mapping to mRatBN7.2 and variant calling, we used the anomalies in the genotype data to further assess the quality of mRatBN7.2. This analysis was performed at two levels to detect issues at both the segment level and the individual nucleotide level.

First, we analyzed segment-wise distribution patterns of heterozygous genotypes and no-calls. Since inbred lines are expected to show a negligible number of heterozygous sites, genomic regions with an unusually high density of heterozygous genotypes may indicate a segment-wise assembly error. For example, if two segments are tandem repeats of each other and have been "folded" into a single segment in the mRatBN7.2 assembly, twice as many reads will map to this region, and will produce a high density of heterozygous sites and multiple-allelic sites, similar to what we have reported as assembly errors in Rnor_6.0[22]. We focused on the 12 BN samples, because BN is the basis of the reference. Along the genome, there are still regions with high heterozygous rates for the 12 BN samples. We applied a custom algorithm to identify regions of these suspected assembly errors. In all, we identified 673 such "flagged regions", with an average length of 52,199 bp, which collectively covered ~1.4% of the genome (Table S7). This rate is much reduced from that of Rnor_6.0[22].

While these regions are defined by using BN samples, a high fraction of heterozygous genotypes for the 151 non-BN samples also fall into them (not shown). Further, among the 151 non-BN samples, some regions of high heterozygosity were observed outside the list of 673 flagged regions. These "anomalies" may reflect genuine structural variants between the strains, not necessarily segment-wide "errors" of the BN-based reference mRatBN7.2. For instance, if a local tandem repeat occurs for one or many of the non-BN strains, but not in the BN, we would observe such high-het regions in the non-BN samples. Since this report is focused on assessing mRatBN7.2, we did not include a comprehensive analysis here.

Second, in addition to the segment level assessment described above, we examined per-site anomalies, especially those outside the flagged regions. One of the unexpected results is that there are sites with Alt/Alt genotypes in most of the 163 strains, including the 12 BN strains, indicating base-level errors in mRatBN7.2.

These shared variant sites consisted of 33,550 SNPs and 95,636 indels (Table S8). Among them,117,901 were homozygous alternative genotypes, and 11,285 were heterozygous in more than 156 samples (Figure S11). The read depth was 32.2 ± 10.1 for homozygous and 66.3 ± 26.2 for heterozygous variants. Because all samples were inbred, the doubling of read depth for the heterozygous variants strongly suggests that they mapped to regions of the reference genome with collapsed repetitive sequences. This is supported by the location of these variants: homozygous SNPs were more evenly distributed, and heterozygous variants were often clustered in a region (Figure 5). These results indicated that many of the potential errors in mRatBN7.2 are caused by the collapse of repetitive sequences.

Functionally, these regions of potential misassembly impact some well-studied genes, such as *Chat, Egfr, Gabrg2, and Grin2a*. The NCBI RefSeq team has referred most of these errors to the GRC for curation. Genes such as *Akap10, Cacna1c, Crhr1, Gabrg2, Grin2a, Oprm1* have been resolved by GRC curators but have not been incorporated into mRatBN7.2 because they will change the coordinates of the reference. After removing the likely errors, we annotated the VCF files resulting from joint variant calling of 163 samples (Table S5) and used these for subsequent analysis.

These site-wise errors are of a different nature than the segment-wise assembly errors, as inaccuracies in the designation of the reference and non-reference alleles do not affect the validity of the site or the segment, rather the analyst needs to be mindful in the tracking of reference alleles, major alleles, and ancestral alleles in downstream analysis.

Complexities in transitioning from Rnor_6.0 to mRatBN7.2

Liftover tools can convert genomic coordinates between different versions of the reference assembly. They rely on a precomputed database of matched genomic segments to return results quickly in a standardized way. However, liftover can only return results for regions with one-to-one matches between the two references. We examined Liftover from Rnor_6.0 to mRatBN7.2 by testing a mock set of variant sites evenly distributed at 1 kb intervals. Of the 2.78 M simulated variants, 92.1% were successfully lifted. Thus ~8% of the Rnor_6.0 genome do not have a unique match in BN7.2. These "unliftable" sites do not distribute evenly along Rnor_6.0 Figure S12, rather they tend to aggregate in regions with no credible match, i.e., lost in BN7.2 Figure S13.

The rate of "liftover loss" varies by the type of genomic feature, and as such will be study-dependent. For example, we used WGS data for one sample to call variants on Rnor_6.0, then lifted them to mRatBN7.2, and compared the results against the variants called directly on mRatBN7.2. Variants called on mRatBN7.2 had a higher proportion (97.99%) of passing the quality filter than those called on Rnor_6.0 (83.64%), and 97.93% of the variants called on Rnor_6.0 were liftable to mRatBN7.2 (Figure 6A). Among the lifted variant sites, 94.48% had a match in the variant set called directly. However, 11.91% of the variants called on mRatBN7.2 were absent in the lifted variant set (Figure 6B). For situations like this, complete remapping of the data to the new reference is preferable despite its time and resource costs, due to the inherent limitation of the liftover process in not being able to assign variants without one-to-one matches.

A comprehensive survey of the genomic landscape of *Rattus norvegicus* based on mRatBN7.2

To facilitate a smooth transition to mRatBN7.2, we conducted the largest joint analysis of WGS data for laboratory rats. We collected WGS for a panel of 163 rats (new data from 127 rats and 36 datasets downloaded from NIH SRA; hereafter referred to as RatCollection, Table S9). RatCollection includes all 30 RI strains of the HXB/BXH family, 25 RI strains in the FXLE/LEXF family, and 33 other frequently used inbred strains. In total, we covered 88 strains. Since some strains have been split into two or more substrains, in all we analyzed 120 samples at the substrain level – approximately 80% of the HRDP.

The mean depth of coverage of these samples was 60.4 ± 39.3. Additional sample statistics are provided in Table S10. After removing the 129,186 variants that were potential errors in mRatBN7.2 (above) and filtering for site quality (qual ≥ 30), 19,987,273 variants (12,661,110 SNPs, 3,805,780 insertions, and 3,514,345 deletions) across 15,804,627 variant sites were identified (Table 2). Across the genome, 89.4% of the sites were bi-allelic and the mean variant density was 5.96 ± 2.20/Kb (mean ± SD). The highest variant density of 30.5/Kb was found on Chr 4 at 98 Mb (Figure S14). Most (97.9 ± 1.4%) of the variants were homozygous at the sample level, confirming the inbred nature of most strains, with a few exceptions (Figure S15).

To analyze the phylogenetic relationships of these 120 strains/substrains, we created an identity-by-state (IBS) matrix using 11,585,238 high-quality bi-allelic SNPs (Table S11). Distance-based phylogenetic trees of all strains and substrains are shown in Figure 6. This phylogenetic tree is in agreement with previous publications [30–33] and matches strain origins. The mean IBS for classic inbred strains was 72.30 ± 2.35%, where BN has the smallest IBS (64.76%).

This phylogenetic tree included all major populations of laboratory rats, such as the eight inbred progenitor strains of the outbred HS rats (ACI/N, BN/SsN, BUF/N, F344/N, M520/N, MR/N, WKY/N, and WN/N). [10] The number of sites with a non-reference allele in each of these strains is shown in Figure 7A; WKY/N contributed the largest number of non-reference alleles (Figure 7B). The distribution of the variant sites from all eight strains across the chromosomes is shown in (Figure 7C). Collectively, these 8 strains accounted for 78.6% of all non-reference alleles in the RatCollection. Conversely, 141,556 of these variant sites were not found in any other strains. Although none of these founder strains are alive today, based on IBS, we identified six living proxies of the HS progenitors that were over 99.5% similar to the original progenitor strains: ACI/EurMcwi, BN/NHsdMcwi, F344/DuCrl, M520/NRrrcMcwi, MR/NRrrc, and

WKY/NHsd (Table S12). Of the remaining strains, the best matches of the remaining strains were much less similar: BUF/Mna was the best approximation (73.6%) to BUF/N, and WAG/RijCrl was the closest (72.0%) to WN/N. These living proxy strains could provide insights to the genetic characteristic of the HS population.

Our phylogenetic tree also included two families of RI rats. The HXB/BXH family was generated from SHR/OlaIpcv and BN-Lx/Cub. Together with their parental strains, we identified 7,520,223 variant sites in this population (Table 2). Approximately 24.1–53.5% of the alleles at these sites of each RI strain were derived from SHR/OlaIpcv. While the majority of the strains were highly inbred, with close to 98% of the variants being homozygous (Figure S16), one exception was BXH2, in which 7.7% of variants were heterozygous (Figure S16), likely due to a recent breeding error. The LEXF/FXLE RI family was generated from LE/Stm and F344/Stm. We discovered 9,183,562 variant sites from the parental strains and 25 strains of this family (Table 2). We expect the final variant count of the entire panel to be similar because both parental strains are included in our analysis. The overall rate of homozygous variants in the FXLE/LEXF family (96.8 ± 2.4%) was lower than in other inbred rats (Figure S16). In particular, 15.6% of the sites from FXLE24 contain heterozygous variants, indicating likely breeding errors.

In addition, our analysis also included sets of two or three strains generated by selective breeding for certain traits, such as the Dahl Salt Sensitive (SS) and Dahl Salt Resistant (SR) strains for studying hypertension. These two strains contain 7,171,447 variant sites compared to mRatBN7.2 (Table 2), with 1,024,283 variants unique to SR and 920,234 variants unique to SS. These strain-specific variants were found throughout the genome (Figure S17). A similar pattern was found for the Lyon Hypertensive (LH), Hypotensive (LL), and Normotensive (LN) rats (Table 2) selected from outbred Sprague-Dawley rats for studying blood pressure regulation. [34] Only 281,972, 289,112, and 262,574 variants were unique to LH, LL, and LN, respectively. In agreement with a prior report, [35] these variants were clustered in a handful of genomic hotspots (Figure S18).

Impact of rat variants on genetic studies of human diseases

We used SnpEff (v 5.0e) to predict the impact of the 19,987,273 variants in the RatCollection based on RefSeq annotation. Among these, 18,646 variants near coding genes were predicted to have a high impact (i.e., causing protein truncation, loss of function, or triggering nonsense-mediated decay, etc.) on 6,667 genes, including 3,930 protein-coding genes (Table S13). The number of genes affected by variants with moderate or low impact variants, as well as detailed functional categories, are provided in Table S13.

Among the predicted high-impact variants, annotation by RGD disease ontology identified 2,601 variants affecting 2,079 genes that were associated with 3,261 distinct disease terms. Cancer/tumor (878), psychiatric (612), intellectual disability (505), epilepsy (319), and cardiovascular (304) comprised the top 5 disease terms, with many genes associated with more than one disease term. A mosaic representation of the number of high-impact variants per disease term for each strain is shown in (Figure S20). The top disease categories for the two RI panels are comparable, including cancer, psychiatric disorders, and cardiovascular disease. The disease ontology annotations for variants in the HXB/BXH, FXLE/LEXF RI panels, and SS/SR, as well as LL/LN/LH selective bred strains, are summarized in Figure S21, Figure S22, Table S14, and Table S15.

We further annotated genes using the human GWAS catalog. [36] Among the rat genes with high-impact variants, 2,034 have human orthologs with genome-wide significant hits associated with 1,393 mapped traits (Table S16). The most frequent variant type among these rat genes was frameshift (1,557 genes), followed by splice donor variant (136 genes) and gain of stop codon (116 genes). Although rats and humans do not share the same variants, strain with these variants can potentially be a useful model for related human diseases at the gene level.

Discussion

We systematically evaluated mRatBN7.2, the seventh iteration of the reference genome for *Rattus norvegicus*, and confirmed that it vastly improved assembly quality over its predecessor, Rnor_6.0. As a result, mRatBN7.2 improved the analysis of omics data sets and now enables powerful and efficient genome-to-phenome analysis of 20 million variants segregating in the laboratory rat. To facilitate the transition to mRatBN7.2, we conducted the largest joint analysis of rat WGS data to date, including 163 samples representing 88 strains and 32 substrains, and identified 15,804,627 variant sites. In addition, our analyses generated additional rat resources such as a genetic map with 150,835 binned markers, a comprehensive rat phylogenetic tree, and a collection of transcription start sites and alternative polyadenylation sites.

Previous references employed slightly different assembly statistics. To enable a direct comparison, we used the methods by VGP [23] to generate comparable measures (Table 1), which indicated significant improvements in mRatBN7.2. Short-read data generated for the reference assembly is often used to evaluate the base-level and segment-level quality. [37] We used a WGS data set containing 36 samples to show that base-level errors were reduced by 9.2 fold in mRatBN7.2. Many methods have been developed to evaluate the structural accuracy of an assembly using sequencing data (e.g.,

QUAST-LG, [38] Merqury [39]). Our evaluation used independent information obtained from a rat genetic map. By comparing the physical distance between 151,380 markers and the order of markers on the reference genomes against their genetic distance calculated based on recombination frequency (Figure 1, Figure S5, S6), we confirmed that most structural differences between Rnor_6.0 and mRatBN7.2 are due to errors in Rnor_6.0. Therefore, mRatBN7.2 is an rat reference genome with improved contiguity as well as increased structural and base accuracy. The improvement in mRatBN7.2 will enhance the quality of rat omics studies. For example, we found improvement of mapping rates, resulting in increased depth of coverage in WGS data. We also noted many qualitative differences that resulted in opposite interpretations (e.g., cis- vs trans-eQTL).

The improvements in mRatBN7.2 are based on new assembly methods and long-read data. [23] However, the PacBio CLR reads used in mRatBN7.2 have lower base accuracy than Illumina short reads. [40,41] Although Illumina data were used to polish the assembly, [23] polishing methods do not correct all base-level errors. [40,42] Our joint analysis of 163 WGS datasets identified 129,186 sites with likely nucleotide errors in mRatBN7.2. Another source of potential error is the assembly method itself. mRatBN7.2 was assembled with VGP pipeline v1.6., [23,43] which assembles the long reads into a diploid genome containing a primary and an alternative assembly. [44] This pipeline is well suited to assemble diploid genomes. When applied to BN/NHsdMcwi, a fully inbred rat, the pipeline classified some duplications with small variants as two haploids, resulting in a collapsed repeat. [45] Although additional data and the applied manual curation can fix most of these errors, the best solution is to create a new telomere-to-telomere (T2T) assembly like the one reported for the human genome. [46]

Liftover enables direct translation of genomic coordinates between different references, thereby reducing the cost of transitioning to a new reference. We found that 92.05% of simulated variants and 97.93% of variants from a WKY/N sample identified on Rnor_6.0 were lifted successfully to mRatBN7.2. This difference is attributable to the large number of simulated variants located in regions of low complexity. While promising, we found that reanalysis of the original sequencing data using mRatBN7.2 discovered an additional 507.7 K variant sites, located primarily in regions not present in Rnor_6.0. Thus, to ensure the best use of past data, remapping to mRatBN7.2 is preferred over using liftover even though the latter is more convenient.

To facilitate the transition for studies of specific rat models, we mapped WGS data of 88 strains (120 substrains and 163 samples) to mRatBN7.2. Joint analysis identified 20.0 million variants from 15.8 million sites. This analysis expanded many prior analyses of rat genomes. For example, Baud et al. [11] analyzed 8 strains against Rnor3.4 and found 7.9 million variants, Atanur et al. [33] analyzed 27 rat strains against Rnor3.4 and reported

13.1 million variants, Hermsen et al. [47] analyzed 40 strains against Rnor5.0 and reported 12.2 million variants. Most recently, Ramdas et al. [22] analyzed 8 strains and reported 16.4 million variants. In addition to using the latest reference genome and an expanded number of strains, our pipeline depends on Deepvariant and GLNexus, which have been shown to improve call set quality, especially on indels. [26,48] Thus, our data provide the most comprehensive analysis of genetic variants in the laboratory rat population to date, and of comparative interest, is twice the variant count of the highly used mouse BXD family [49,50].

This collection of rats represented a wide variety of rats that are used in genetics studies today. For example, our analysis included the full HXB/BXH panel and 27 strains/substrains of the FXLE/LEXF RI panel. Together with the inbred strains, they cover about 80% of the rats in the HRDP. [51] The new variant set from our analysis provide a much-needed boost in mapping precision: prior mapping of these RI families was based on several hundred to tens of thousands markers. [8,51,52]

The outbred N/NIH HS rats are another widely used rat genetic mapping population. [13] Our analysis is in agreement with Ramdas et al. [22] in identifying 16 million variants in the progenitors. Updated genetic data will be useful in HS genetic mapping studies, such as for the imputation of variants. Although live colonies of the original NIH HS progenitor strains are no longer available, we identified 6 living substrains that are genetically almost identical to the original progenitors (99.5% IBS), while the closest match to the other two strains has IBS of approximately 70% (Table S12). These living substrains will be useful in many ways, such as studying the effect of variants identified in genetic mapping studies. Our analysis also included groups of inbred rats segregated by less than 2 million variants. For example, the LH/LN/LL family , [34,35] and the SS/SR family (Table S13), as well as several pairs of near isogenic lines with distinctive phenotypes. These rats can be exploited to identify causal variants using reduced complexity crosses. [53]. Updated genotyping data for these populations will benefit all ongoing studies that use these rats.

A large trove of phenotypic and genomic data have been collected from laboratory rats in the past decades. For example, studies using RI panels have identified loci that control a range of physiological and pathological phenotypes, such as cardiovascular disease, [54] hypertension, [55,56] diabetes, [57] immunity, [57] tumorigenesis, [58] and tissue specific gene expression profiles. [59] Using the outbred HS rats, Baud et al. [11] reported 355 QTL in a study that measured 160 phenotypes representing six diseases and risk factors for common diseases. Other studies using the HS population has revealed genetic control of behavior, [15,60] obesity, [61] and metabolic phenotypes. [62] Many of these

phenotypic data are available from the RGD. [16] While all these data were analyzed using previous versions of the reference genome, reanalysing them using updated genomic data could lead to novel discoveries. [63]

By generating F_1 hybrids from these inbred lines with sequenced genomes, novel phenotypes can be mapped onto completely defined genomes: the 82 sequenced HRDP strains can produce any of 6,642 isogenic but entirely replicable F_1 hybrids with completely defined genomes. Studies of these "sequenced" F_1 hybrids avoid the homozygosity of the parental HRDP strains and enable a new phase of genome-phenome mapping and prediction. [49] While several genetic mapping studies using the HRDP are currently underway, the large number of variants in the HRDP (c.f., the hybrid mouse diversity panel contains about 4 million SNPs [64]) and WGS-based genotype data will further encourage the use of this resource.

We used SnpEff to evaluate the potential functional consequences of these variants. We identified 18,646 variations likely to have a high impact on 6,667 genes, and many more variants predicted to have regulatory effects on gene expression (Table S12). While the majority of these predictions have not been verified experimentally, some are strongly supported by the literature. For example, the SS rats develop renal lesions with hypertension, and have high impact mutations in *Capn1* [65] and *Procr*, [66] both associated with kidney injuries, as well as in *Klk1c12*, associated with hypertension. [67] These annotations identified many genes with variants that either result in a gain of STOP codon or cause a frameshift, which could lead to the loss of function (LoF). As exemplified in a recent work, [68] strains harboring these variants can be explored to investigate the function of these genes. Further, a near-complete catalog of strain-specific alleles and functional prediction is a stable source of potential candidate variants for interpreting genetic mapping results.

These functional annotations are highly relevant when the human orthologue of these genes is associated with certain traits in human GWAS (Table S15). For example, CDHR3 is associated with smoking cessation. [69] A gain of STOP mutation in the *Cdhr3* gene was found in only one parent of both RI panels (SHR/OlaIpcv and LE/Stm). Using these RI panels to study the reinstatement of nicotine self-administration, a model for smoking cessation, will likely provide insights into the role of CDHR3 in this behavior. Further, a near-complete catalog of strain-specific alleles and functional prediction provide a stable source of potential candidate variants for interpreting genetic mapping results.

Our phylogenetic analysis agrees with those published previously. [30,33] Our phylogenetic analysis included the HXB/BXH and FXLE/LEXF RI panels, along with other inbreds.

Genetic relationships between strains in the RI panels can provide insights strain selection is needed when designing studies. Our phylogenetic analysis confirmed that BN/NHsdMcwi, the reference strain for *Rattus norvegicus*, is an outgroup to all other common laboratory rats (Figure 6). This is consistent with its derivation from a pen-bred colony of wild-caught rats [3] and previous studies that included wild rats. [32] Thus, mapping sequence data from other strains to the BN reference yields a greater number of variants (but at slightly reduced mapping quality) than using a hypothetical reference that is genetically closer to the commonly used laboratory strains. This so-called reference bias has been observed in genomic [70] and transcriptomic data analyses. [71] While alternative reference strains can be selected, it should be noted that no individual strain is a perfect representation of a population. Instead, the nascent field of pangenomics, [72] where the genome of all strains can be directly compared to each other, provides a promising future where all variants can be compared between individuals directly without the use of a single reference genome. This pangenomic approach will be especially powerful when individual genomes are all assembled from long-read sequence data, some of which are already available. [73] This will enable a complete catalog of all genomic variants, including SVs and repeats, that differ between individuals.

In addition to WGS data and analysis, our analysis also generated other rat genomic resources. This includes a new rat genetic map with 150,835 markers. By providing the centimorgan distances and the order of these markers to the community, we envision this map will have multiple applications. For example, instead of being used for assembly evaluation, this map can be integrated into the de novo assembly process, as demonstrated by the new assembly of the stickleback genome. [74,75]. Unlike human and mouse genomes [76], functional elements in the rat remain poorly annotated. Our analysis produced a list of TSS locations for genes expressed in the prefrontal cortex or nucleus accumbens (Table S5); APA sites of genes expressed in the brain based on sequencing whole transcriptome termini sites (Table S5). These new data sets will further the study of gene regulatory mechanisms in rats.

Research using the *Rattus norvegicus* has made significant contributions to the understanding of human physiology and diseases. An updated reference genome provides a valuable resource not only for future studies using laboratory rats to understand the genetics of human disease, but also opportunities for analyzing existing data to gain new insights. The rich literature on physiology, behavior, and disease models in laboratory rats, combined with the complex genomic landscape revealed in our survey, demonstrates that the rat is an excellent model organism for the next chapter of biomedical research.

Acknowledgments

The work of PR is supported by the Academy of Finland (grant number 343656). The work of MT is supported by NIH NHLBI R01HL064541, P01HL149620, and Office of the Director R24OD024617. The work of HA is supported by NIH NIDA U01DA043098. The work of CB is supported by NIH NIDA U01DA051972. The work of WMD is supported by NIH NHLBI R01HL064541 and Office of the Director R24OD024617. The work of AMG is supported by NIH NHLBI P01HL149620 and Office of the Director R24OD024617. The work of TH is supported by Wellcome Trust [WT222155/Z/20/Z]. The work of TK is supported by NIH R01HG011252. The work of FJM is supported by Wellcome Trust [WT222155/Z/20/Z]. The work of PM is supported by NIH R01GM140287. The work of MP is supported by a program from the National Institute for Research of Metabolic and Cardiovascular Diseases (Program EXCELES, ID Project No. LX22NPO5104) funded by the European Union – Next Generation EU. The work of JS is supported by NIH NIDA U01DA051234. The work of JRS is supported by NIH NHLBI R01HL064541, NHGRI U24HG010859, and Office of the Director R24OD024617. The work of LCS and HS rats is supported by NIH NIDA P50DA037844. The work of BT is supported by NIH NIAAA R24AA013162. The work of FT is supported by NIH NIDA U01DA050239 and U01DA051972. The work of LS is supported by NIH NIDA P30DA044223. The work of TDM is supported by the National Center for Biotechnology Information of the National Library of Medicine (NLM), National Institutes of Health. The work of AEK is supported by NIH NHLBI R01HL064541, P01HL149620, NHGRI U24HG010859, and Office of the Director R24OD024617. The work of MRD and HRDP is supported by NIH Office of the Director grant R24OD024617. The work of RWW is supported by NIH NIDA U01DA047638 and P30DA044223. The work of JZL is supported by NIH NIDA U01DA043098. The work of HC is supported by NIH NIDA U01DA047638, P50DA037844, and R01DA048017.

Author contributions

Conceptualization, A.A.P. R.W.W. J.Z.L. H.C.; Formal Analysis, T.V.d. Y.P. P.R. D.M. M.T. X.W. T.D.M. J.Z.L. H.C.; Visualization, T.V.D. Y.P. P.R. D.M. F.T. Z.J. L.S. X.W. J.Z.L.; Investigation, H.A. C.B. D.C. A.S.C. W.C. V.C. W.M.D. P.A.D. E.G. A.M.G. H.M.G. V.G. T.H. K.H. J.H. T.K. P.K. L.L. S.M. F.J.M. P.M. A.B.O. O.P. P.P. J.S. J.R.S. L.C.S. B.T. A.T. M.U. F.V. H.W. F.T. Z.J. L.S.; Resources, C.L.D. M.P. A.E.K. M.R.D.; Data Curation, W.M.D. A.M.G. J.R.S. A.E.K. M.R.D.; Writing - Original Draft, T.V.d. Y.P. P.R. D.M. T.H. L.S. X.W. T.D.M. J.Z.L. H.C.; Writing - Review & Editing, A.M.G. B.M.S. L.S. X.W. T.D.M. A.A.P. A.E.K. M.R.D. R.W.W. J.Z.L. H.C.; Supervision, J.Z.L. H.C.

Declaration of interests

The authors declare no competing interests.

Figure Legends

Figure 1. mRatBN7.2 corrects structural errors in Rnor_6.0. (A) Genome-wide comparison between Rnor_6.0 and mRatBN7.2 showed many structural differences between these two references, such as a large inversion at proximal Chr 6 and many translocations between chromosomes. Image generated using the NCBI Comparative Genome Viewer. Numbers indicate chromosomes. Green lines indicate sequences in the forward alignment. Blue lines indicate reverse alignment. **(B)** The large inversion on proximal Chr 6 is shown in a dot plot between Rnor_6.0 and mRatBN7.2. **(C)** A rat genetic map generated using 150,835 binned markers from 1,893 heterogeneous stock rats showed an inversion at proximal Chr 6 between genetic distance and and physical distance based on Rnor_6.0, indicating the inversion is caused by assembly errors in Rnor_6.0. **(D)** Marker order and genetic distance from the genetic map on Chr 6 are in agreement with physical distance based on mRatBN7.2, indicating the misassembly is fixed. **(E-G)** Genetic map confirms many assembly errors on Chr 19 in Rnor_6.0 are fixed in mRatBN7.2.

Figure 2. mRatBN7.2 improved mapping statistics of whole-genome sequencing data. Summary statistics from mapping 36 HXB/BXH WGS samples against Rnor_6.0 and mRatBN7.2 were compared. Using mRatBN7.2 increased percentage of reads mapped **(A)**, reduced percentage of regions on the reference genome with zero coverage **(B)**, total number of SNPs **(C)** and indels **(D)**. The presence of a large number of SNPs **(E)** and indels **(F)** that are shared by all samples (arrows), including BN/NHsdMcwi, indicating they are base-level errors in the reference genome.

Figure 3. mRatBN7.2 improves eQTL analysis. Genome misassembly is associated with increased rates of calling spurious trans-eQTLs. We compared eQTL mapping using an existing RNA-seq data from nucleus accumbens core. (**A)** Each column represents a gene for which at least one trans-eQTL was found at P<1e-8 using Rnor_6.0. The color of bars indicate the number of trans-eQTL SNP-gene pairs in which the SNP and/or gene transcription start site (TSS) relocated to a different chromosome in mRatBN7.2, and whether the relocation would result in a reclassification to cis-eQTL (TSS distance <1 Mb) or ambiguous (TSS distance 1-5 Mb). **(B)** Genomic location of one relocated trans-eQTL SNP from (A). The SNP is in a segment of Chr 13 in

Rnor_6.0 that was relocated to Chr 3 in mRatBN7.2 (red stars), reclassifying the e-QTL from trans-eQTL to cis-eQTL for both *Ly75* and *Itgb6* genes (red bars).

Figure 4. mRatBN7.2 improves the analysis of proteomic data. We compared protein identification and pQTL mapping using a brain proteome data. **(A)** Histogram showing the distance between cis-pQTLs and transcription starting site (TSS) of the corresponding proteins. The distances of pQTLs in mRatBN7.2 tend to be closer than those in Rnor_6.0. **(B)** An example of trans-pQTL in Rnor_6.0 was detected as a cis-pQTL in mRatBN7.2. **(C)** Correlation of expression of the protein (the example in panel B) in Rnor_6.0 and mRatBN7.2. **(D)** Different annotations of the exemplar gene in Rnor_6.0 and mRatBN7.2.

Figure 5. SNPs and indels indicate remaining errors in mRatBN7.2. Base-level errors are indicated by homozygous variants that are shared by the majority (i.e. more than 153 out of 163) of samples, including all seven BN/NHsdMcwi rats, one of them is part of the data used to assemble mRatBN7.2. Variants that are heterozygous for the majority of the samples are clustered in a few regions and have significantly higher read-depth. This suggests that they originated from collapsed repeats in mRatBN7.2.

Figure 6. Phylogenetic relationship of 120 strain/substrains of laboratory rats. The phylogenetic tree was constructed using 11.6 million biallelic SNPs from 163 samples. Strains/substrains with duplicated samples were condensed. Strains highlighted with bold fonts are parental strains for RI panels. Green: HXB/BXH RI panel. Blue: FXLE/LEXF RI panel. Orange: progenitors of the HS outbred population.

Figure 7. **Genetic diversity among progenitors of heterogeneous stock (HS) rats.** **(A)** The HS progenitors contain 16,438,302 variants (i.e., 82.2% of the variants in our collection of 120 strain/substrains) based on analysis using mRatBN7.2. Among these, 10,895 are shared by all eight progenitor strains. The number of variants that are unique to each specific founder is noted. (**B)** The total number of variants per strain, with the total number unique to each strain marked. (**C)** The number of variants shared across N strains, shown per chromosome.

Figure 8. Using WGS data to assess the quality of the LiftOver. LiftOver is a tool often used to translate genomic coordinates between versions of reference genomes. We evaluated the effectiveness of LiftOver from Rnor_6.0 to mRatBN7.2. **(A)** Overview of the workflow using a real WGS sample from a WKY rat. A higher portion of variants passed the quality filter for mRatBN7.2. Among them, 97.93% of the variants were liftable from Rnor_6.0 to mRatBN7.2. **(B)** The overlap between variants lifted from Rnor_6.0 and variants obtained by direct mapping sequence data to mRatBN7.2. Approximately 11.9% of the variants that were found from direct mapping were missing from the LiftOver.

Tables

Table 1. Global statistics for the Rat, Mouse, and Human reference genomes. Genomes are downloaded from UCSC Goldenpath. Summary statistics are calculated based on the fasta files of each release using QUAST.

	Rnor_6.0	mRatBN7.2	GRCm39	GRCh38	CHM13
Year published	2014	2021	2020	2014	2021
Total sequence length	2,870,182,909	2,647,915,728	2,728,222,451	3,209,286,105	3,054,832,041
Total ungapped length	2,729,984,219	2,626,580,772	2,654,621,837	3,049,316,098	3,054,832,041
Number of scaffolds	953	176	61	455	24
Scaffold N50	145,729,302	135,012,528	130,530,862	145,138,636	154,259,566
Scaffold L50	8	8	9	9	8
Number of contigs	75695	757	347	1431	24
Contig N50	100,511	29,198,295	59,462,871	56,413,054	154,259,566
Contig L50	7,346	27	15	19	8
Total number of chromosomes and plasmids	23	23	22	25	24

Table 2. Genetic variants in laboratory populations. The RatCollection includes 163 rats (88 strains and 32 substrains, with some biological replicates). The HRDP contains the HXB/BXH and FXLE/LEXF panels as well as 30 or so classic inbreds. Our analysis includes ~80% of the HRDP. The variants were jointly called using Deepvariant and GLNexus. Variant impact was annotated using SnpEff. * Variants that are combinations of insertions, deletions or SNPs. † Including parental strains.

	Variants sites	Variants	Variant Type			Predicted Impact			Alt/Alt Homozygous %(mean±SD)	Genotype Qual (mean±SD)
			SNPs	Indels	Mixed*	High	Low	Moderate		
RatCollection	15,804,627	19,987,273	12,661,110	7,313,702	12,461	18,646	262,685	125,523	97.9±1.4	70.1±21.2
HS progenitors	12,418,243	16,438,302	9,947,112	6,479,485	11,705	6,980	205,316	94,659	98.5±0.3	71.4±22.0
FXLE/LEXF†	9,183,562	13,070,345	7,036,182	6,023,391	10,772	13,988	143,623	66,186	96.8±2.4	72.3±21.0
HXB/BXH†	7,520,223	11,256,227	5,705,592	5,541,195	9,440	10,121	115,081	53,819	97.9±1.2	72.2±22.8
SS/SR	7,171,447	10,522,763	5,544,220	4,969,398	9,145	8,606	111,658	51,149	98.0±0.9	72.3±21.8
LL/LN/LH	6,923,575	10,112,755	5,433,556	4,670,291	8,908	4,142	111,040	52,364	98.5±0.3	73.2±21.4

Methods

Data availability. The RatCollection contains 163 WGS samples from 88 strains and 32 substrains. It includes new data from 127 rats and 36 datasets downloaded from NIH SRA. The detailed sample metadata are provided in Table S9. The Hybrid Rat Diversity Panel (HRDP) consists of 96 inbred strains, and includes 30 classic inbred strains and both of the large RI families discussed in the prior sections (BXH/HXB and LEXF/FXLE). The panel is being cryo-resuscitated and cryopreserved at the Medical College of Wisconsin for use by the scientific community. A total of 82 members of the HRDP have been sequenced using Illumina short-read technology, including all 30 extant HXB strains, 23 of 27 FXLE/LEXF strains, and 25 of 30 classic inbred strains. RatCollection includes all 30 strains of the HXB/BXH family, 27 strains in the FXLE/LEXF family, and 33 other inbred strains. In total, we covered 88 strains and 32 substrains. It contains approximately 80% of the HRDP. WGS data generated for this work are been uploaded to NIH SRA (see Table S8 for SRA IDs). Additional resources are listed in Table S5.

Code availability. The code for the custom R, Python and Bash scripts for data analysis is available upon request.

Lead contact. Hao Chen (hchen@uthsc.edu). Any additional information required to reanalyze the data reported in this paper is available from the lead contact upon request.

Calculating genome assembly statistics. We obtained all assemblies from UCSC Goldenpath, with the exception of CHM13_T2T_v1.1, which was downloaded from the T2T Consortium GitHub page. We used QUAST to calculate common assembly metrics, such as contig and scaffold N50 (Mikheenko et al., 2018), using a consistent standard across all assemblies. We defined each entry in the fasta file as a scaffold, breaking them into contigs based on continuous Ns of 10 or more. No scaffolds below a certain length were excluded from the analysis. [23] Our scripts and intermediate results can be found in the supplementary. Nx plots were generated using a custom Python script and the fasta files as inputs. Structural differences between Rnor_6.0 and mRatBN7.2 were evaluated using paftools. [77]

Analysis of WGS data. We used different methods for mapping data, based on the sequencing technologies. For illumina short read data, fastq files were mapped to the reference genome (either Rnor_6.0 or mRatBN7.2) using BWA mem. [78] GATK [79] was then used to mark PCR duplicates in the bam files. For 10x chromium linked reads, fastq files were mapped against the reference genomes using LongRanger (version

2.2.2). Long read data were mapped using Minimap2, [80] Deepvariant [25] (ver 1.0.0) was then used to call variants for each sample. Joint calling of variants for all the samples was conducted using GLNexus. [26] Large SVs detected by LongRanger were merged using SURVIVOR [81] per reference genome. SVs detected in less than two samples were removed. Variants with the QUAL score less than 30 were removed. The impact of variants were predicted using SnpEff, [82] using RefSeq annotations. Overlap between SNPs and repetitive regions were identified with RepeatMasker. [83] Disease ontology was retrieved from the Rat Genome Database. [16] Disease associations were related to nearest genes as predicted by SnpEff. Subsequent analyses were conducted using custom scripts in R or bash. Circular plots were generated with the Circos plots package in R. Functional consequences of variants on genes were searched in PubMed via GeneCup. [84]

Sample quality control. To ensure the quality of data from 168 rats, we conducted a thorough examination of the missing call rate and read depth per sample. We determined that a per sample missing rate of 4% and average read depth of 10 were appropriate based on the data distribution. We identified and removed 4 samples with high missing rates (SHR/NCrlPrin_BT.ILM, WKY/NHsd_TA.ILM, GK/Ox_TA.ILM, FHL/EurMcwi_TA.ILM) and 2 samples with low read depth (WKY/NHsd_TA.ILM, BBDP/Wor_TA.ILM), resulting in a total of 5 samples removed.

Identification of genomic regions with potential mis-assembly in mRatBN7.2. We used WGS-derived genotype data for 163 samples to detect genomic regions with unusually high densities of heterozygous genotypes (i.e., the "high-het" regions). Since the samples are from inbred animals, high-het regions could arise from tandemly repeated segments in the BN genome "folded" into a single region in mRatBN7.2. While read-depth data represent an independent source of information, here we focused on the distribution patterns of heterogeneous genotypes in the 12 BN animals. Indeed, along the genome, the per-site heterozygote counts, ranging 0 to 12 across the 12 BN samples, tend to be high in certain discrete regions, which also tend to have high counts of NA (the "no-calls"). We used the het+NA counts as the scanning statistics for segment-wise switches between a high-state and a low-state, akin to using arrayCGH intensity data or sequencing read depths to detect DNA copy-number variants (CNVs). Specifically, we added 2 to the per-site het+NA counts, to mimic the situation with 2 DNA copies in baseline regions and up to 14 copies in the high-regions. The logged values, ranging from log2(2) to log2(14), are "segmented" by using the segment command in R package "DNAcopy", with parameters min.width=5,alpha=0.001. The results tend to be over-segmented, and they are merged by a custom R script with the following merging rules. Starting from the first three segments, we merge the first and

the second segments if one of the four conditions are met: (1) both have mean values above 1.5, which is an empirically derived threshold in our log2(x+2) scale, (2) both have mean values below 1.5, (3) the three segments are high-low-high but the middle segment is less than 5 kb, hence a "positive flicker", or (4) the three segments are low-high-low with the middle segment shorter than 5 kb: a "negative flicker". If the first two segments are merged, the next "triplet" to be evaluated are the merged 1-2, the previous #3 segment, and the newly called-up $4 segment. If no merging is executed, the scan moves by one segment to evaluate the next "triplet": #2-4. This operation was repeated until we reach the end of the chromosome. Altering the merging parameters will yield a somewhat different set of "flagged" regions. The current merged list contains 673 high-segments over the 20 autosomes, covering about 1.4% of mRatBN7.2 and having an average length of 52,199 nt. Future iterations will incorporate distribution patterns of read depth, multi-allelic sites and, if possible, linked read information. Similar scans can be performed for the 151 non-BN samples. Our preliminary data show that most of the regions flagged by the 12 BN samples also show high Het+NA counts in non-BN samples. In addition, some other heterozygous genotypes in non-BN samples fall outside the flagged regions, either individually or in new segments not flagged in BN samples. Many of them likely represent single-site or segment-wise differences between these strains and the reference strain: BN, and they may vary in a strain-specific fashion.

Evaluating Liftover. The Liftover too is evaluated using both simulated and real data. The simulated data is an evenly 1000-base pair-spaced bed file covering Rnor_6.0 (2,782,023 sites within the bed file). The simulated dataset is used to study what portion of the genome is liftable, and the distribution of the unliftable and liftable sites. The reall dataset is used to evaluate the accuracy and utility of the Liftover process, we compared the variants obtained through the Liftover process to those directly called from the data. We mapped WGS data from a WKY/N rat to both Rnor_6.0 and mRatBN7.2 and called variants against each respective genome. We then used the UCSC Liftover tool [85] and corresponding chain files to lift these variants to the other reference genome. The resulting lifted variant sets are then compared to the directly called variant sets.

Identify live strains that are close to HS progenitors. Currently, there are two colonies of the HS rats: one located at Wake Forest University (RRID:RGD_13673907), which was moved from the Medical College of Wisconsin (RRID:RGD_2314009); the University of California San Diego houses the other colony (RID:RGD_155269102). While the original progenitor population is no longer alive, we obtained DNA samples that were preserved in 1984, when the HS colony was created. Using the 163-by-163

IBS matrix previously generated (see method: tree generation). We identified six closely-related substrains of the progenitors that were over 99.5% similar to the original strains based on identity by state (IBS): ACI/EurMcwi, BN/NHsdMcwi, F344/DuCrl, M520/NRrrcMcwi, MR/NRrrc WKY/NHsd. The best matches of the remaining strains were less similar: BUF/Mna (73.6%) for BUF/N and WAG/RijCrl (72.0%) for WN/N. Better alternatives for these two strains may be identified in the future as more inbred rat strains are sequenced. At the time of this report, all 8 of these inbred strains are available from Hybrid Rat Diversity Program at the Medical College of Wisconsin (see https://rgd.mcw.edu/wg/hrdp_panel/ for strain availability and contact details).

Constructing a genetic map using genetic data from a large HS cohort. The collection of genotypes from 1893 HS rats and 753 parents (378 families) was described previously. [15] Briefly, genotypes were determined using genotyping-by-sequencing. [86] This produced approximately 3.5 million SNP with an estimated error rate <1%. Variants for X- and Y-chromosomes were not called. The genotype data used for this study can be accessed from the C-GORD database at doi: 10.48810/P44W2 or through https://www.genenetwork.org. The genotype data were further cleaned to remove monomorphic SNPs. Genotypes with high Mendelian inheritance error rates (>2% error across the cohort) were identified by PLINK [87] and removed. We further used an unbiased selection procedure, which yielded a final list of 150,835 binned markers distributed across the genome. Mean distance between markers is 18.5 kb across the genome. We used Lep-MAP3 (LM3) [88] to construct the genetic map. The following LM3 functions were used: 1) the ParentCall2 function was used to call parental genotypes by taking into account the genotype information of grandparents, parents, and offspring; 2) the Filtering2 function was used to remove those markers with segregation distortion or those with missing data using the default setting of LM3; and 3) the OrderMarkers2 function was used to compute cM distances (i.e., recombination rates) between all adjacent markers per chromosome. The resulting map had consistent marker order that supported the mRatBN7.2.

Phylogenetic tree. We used bcftools [89] to filter for high-quality, bi-allelic SNP sites from the VCF files for the 20 autosomes. We then employed PLINK [87] to calculate a pairwise identity-by-state (IBS) matrix using the 11.5 M variants. We imported the resulting matrix into R and converted it to a meg format as described in the MEGA manual. We then used MEGA [90] to construct a distance-based UPGMA tree using the meg file as input. We also manually adjusted the position of a few internal nodes for improved visualization using the MEGA GUI. The modified tree was exported as a nwk file. We then imported this nwk file into R and used the ggtree [91] package to plot the phylogenetic tree.

RNA-seq data. RNA-seq data was downloaded from RatGTEx. [29] Brains were extracted from 88 HS rats. Rats were housed under standard laboratory conditions. Rat brains were extracted and cryosectioned into 60 µm sections, which were mounted onto RNase-free glass slides. Slides were stored in -80°C until dissection and before RNA-extraction post dissection. AllPrep DNA/RNA mini kit (Qiagen) was used to extract RNA. RNA-seq was performed on mRNA from each brain region using Illumina HiSeq 4000 to obtain 100 bp single-end reads for 435 samples. RNA-Seq reads were aligned to the Rnor_6.0 and mRatBN7.2 genomes from Ensembl using STAR v2.7.8a. [92]

eQTL relocation analysis. We obtained the nucleus accumbens core (NAcc, 75 samples) eQTL dataset from RatGTEx [29] (https://ratgtex.org), which was mapped using Rnor_6.0. We considered associations with p<1e-8 between any observed SNP and any gene. We labeled those for which the SNP was within 1Mb of the gene's transcription start site as cis-eQTLs, and those with TSS distance greater than 5Mb, or with SNP and gene on different chromosomes, as trans-eQTLs. SNP-gene pairs with TSS distance 1-5Mb were not counted in either group. We estimated the set of cross-chromosome genome segment translocations between Rnor_6.0 and mRatBN7.2 using minimap2 [80] with the “asm5” setting. Examples of the relocations were visualized using the NCBI Comparative Genome Viewer (https://ncbi.nlm.nih.gov/genome/cgv/).

Capped small (cs)RNA-seq data. csRNA-seq data used for the alignment metrics were previously published. [93] Briefly, small RNAs of ~15–60 nt were size selected by denaturing gel electrophoresis starting from total RNA extracted from 14 rat brain tissue dissections. For csRNA libraries, cap selection was followed by decapping, adapter ligation, and sequencing. For input libraries, 10% of small RNA input was used for decapping, adapter ligation, and sequencing. After library quality check by gel electrophoresis, the samples were sequenced using the Illumina NextSeq 500 platform using 75 cycles single end. Sequencing reads were aligned to the Rnor_6.0 and rat mRatBN7.2 genome assembly using STAR v2.5.3a [92] aligner with default parameters. Transcriptional start regions were defined using HOMER’s findPeaks tool. [94]

Single nuclei (sn) RNA-seq data. snRNA-seq data used for the alignment metrics were obtained from rat amygdala using the Droplet-based Chromium Single-Cell 3’ solution (10x Genomics, v3 chemistry), as previously described [95]. Briefly, nuclei were isolated from frozen brain tissues and purified by flow cytometry. Sorted nuclei were counted and 12,000 were loaded onto a Chromium Controller (10x Genomics). Libraries were generated using the Chromium Single-Cell 3′ Library Construction Kit v3 (10x Genomics, 1000075) with the Chromium Single-Cell B Chip Kit (10x Genomics,

1000153) and the Chromium i7 Multiplex Kit for sample indexing (10x Genomics, 120262) according to manufacturer specifications. Final library concentration was assessed by Qubit dsDNA HS Assay Kit (Thermo-Fischer Scientific) and post library QC was performed using Tapestation High Sensitivity D1000 (Agilent) to ensure that fragment sizes were distributed as expected. Final libraries were sequenced using the NovaSeq6000 (Illumina). Sequencing reads were aligned to the Rnor_6.0 and rat mRatBN7.2 genome assembly using Cell Ranger 3.1.0.

Transcriptome termini site sequencing

Mapping of alternative polyadenylation sites to the mRatBN7.2 reference genome. A total of 83 WTTS-seq (whole transcriptome termini site sequencing [28]) libraries were constructed individually using total RNA samples derived from several brain tissues of rats. Library sequencing produced a total of 312,092,803 raw reads, but the mapped reads were 240,225,046 (76.97%) on Rnor6.0, while 251,188,567 (80.49%) on mRatBN7.2, respectively. Using 25 reads per clustered site as a cutoff, we identified 173,124 APA sites mapped to the new reference genome, while 167,136 APA sites were assigned to the old reference genome. For Rnor6.0, only 127,460 (76.26%) APA sites were assigned to the genome regions with 18,177 annotated genes. In contrast, 141,399 (81.67%) APA sites were mapped to the 20,102 annotated genes on mRatBN7.2. In brief, our results provide evidence that mRatBN7.2 has improved qualities of both genome assembly and gene annotation in rat.

Brain proteome data. Deep proteome data were generated using whole brain tissue from both parents and 29 members of the HXB family, one male and one female per strain. Proteins in these samples were identified and quantified using the tandem-mass-tag (TMT) labeling strategy coupled with two-dimensional liquid chromatography-tandem mass spectrometry (LC/LC-MS/MS). We used the QTLtools program [96] for protein expression quantitative trait locus (pQTL) mapping. cis-pQTL are defined when the transcriptional start sites for the tested protein are located within ± 1 Mb of each other.

Supplementary Methods

Identifying potentially mislabeled samples. Phylogenetic analysis identified that the metadata of 15 samples contradicted their genetic relationships . These contradictions could happen at many steps during breeding, samples collection, sequencing, or data analysis and the true source is difficult to pinpoint. An advantage of having multiple

biological samples for each strain is that these inconsistencies can be identified. One of the 15 samples is mislabeled and the correct label can be inferred (sample name denoted with ***); two samples are mislabeled and the correct labels cannot be inferred (sample names denoted with **); 12 samples are potentially mislabeled (sample names denoted with *). Details of these samples are described below:

1) There is enough evidence to indicate that this sample is mislabeled, and we can conclusively infer what the true label is. One sample falls into this category: F344/Stm_HCJL.CRM. Despite being named F344, this sample has less than 70% IBS with the other 14 F344 samples, yet has about 99% IBS with 2 LE samples from different institutes (Table S11). We think this sample is mislabeled as F344, and the true label should be LE. Therefore, we changed the sample name accordingly and appended *** to the end of the sample name to denote such a change has been made.

2) There is enough evidence to indicate that this sample is mislabeled, but we cannot conclusively infer what the true label is. Two samples fall into this category: LE/Stm_HCJL.CRM has about 83% IBS with the other 3 LE samples from different institutes (Table S11). The identity of this sample is likely one of the LEXF or FXLE recombinant inbred, but there isn't another sample that has high IBS with it. We think this sample is mislabeled, but the true label is unknown. WKY/Gla_TA.ILM is a sample we downloaded from SRA. This WKY substrain (WKY/Gla) clusters closer to SHR strains than other WKY substrains. The same pattern was also observed in one prior study, [33] and was thought to be caused by the incomplete inbreeding before sample distribution. To further investigate this, we performed regional similarity analysis and found that the pattern observed is consistent with that of a congenic strain created by using SHR as the recipient and WKY as the donor. A literature search confirmed that such strains were indeed once created at the same institute from where WKY/Gla was derived. [97]. We think this sample is mislabeled, but we don't know what the correct label should be.

3) There is evidence to suggest that this sample could potentially be mislabeled, but evidence is not conclusive. A total of 12 samples fall in this category. The majority of the samples of the same substrain but sequenced by different institutes have IBS over 99%; however, we observed a few instances of unexpected low IBS between samples of the same strain but with unexpected high IBS between samples of a different strain. These could be caused by the mis-labeling at either of the institutes. Although we think these samples are at the risk of being mislabeled, it is also possible that individual differences with these strain/substrain could be a cause of the unexpected IBS values. For example, both 7.7% of the variants of the BXH2 samples are heterozygous, while the rate of heterozygosity in the LEXF/FXLE in general is higher than the rest of the inbred strains. These pairs include (Table S11):

- BXH2_MD.ILM & BXH2_HCRW.CRM: unexpected low IBS at 92%

- LEXF4_MD.ILM & LEXF5_HCJL.CRM: unexpected high IBS at 99%
- LEXF3_MD.ILM & LEXF4_HCJL.CRM: unexpected high IBS at 99%
- LEXF1A_MD.ILM & LEXF1C_HCJL.CRM: unexpected high IBS at 99%
- LEXF1C_MD.ILM & LEXF2A_HCJL.CRM: unexpected high IBS at 99%
- LEXF2B_MD.ILM & LEXF1A_HCJL.CRM: unexpected high IBS at 98%
- LEXF4_MD.ILM & LEXF4_HCJL.CRM: unexpected low IBS at 83%
- LEXF1A_MD.ILM & LEXF1A_HCJL.CRM: unexpected low IBS at 84%
- LEXF1C_MD.ILM & LEXF1C_HCJL.CRM: unexpected low IBS at 95%

Ensembl Annotation Annotation of the assembly was created via the Ensembl gene annotation system. [98] A set of potential transcripts was generated using multiple techniques: primarily through alignment of transcriptomic data sets, cDNA sequences, curated evidence, and also through gap filling with protein-to-genome alignments of a subset of mammalian proteins with experimental evidence from UniProt. [99] Additionally, a whole genome alignment was generated between the genome and the GRCm39 mouse reference genome using LastZ and the resulting alignment was used to map the coding regions of mouse genes from the GENCODE reference set.

The short-read RNA-seq data was retrieved from two publicly available projects; PRJEB6938, representing a wide range of different tissue samples such as liver or kidney, and PRJEB1924 which is aimed at understanding olfactory receptor genes. A subset of samples from a long-read sequencing project PRJNA517125 (SRR8487230, SRR8487231) were selected to provide high quality full length cDNAs.

From the 104 Ensembl release annotation on the rat assembly Rnor_6.0, we retrieved the sequences of manually annotated transcripts from the HAVANA manual annotation team. These were primarily clinically relevant transcripts, and represented high confidence cDNA sequences. Using the *Rattus norvegicus* taxonomy id 10116, cDNA sequences were downloaded from ENA and sequences with the accession prefix ‘NM’ from RefSeq. [100]

The UniProt mammalian proteins had experimental evidence for existence at the protein or transcript level (protein existence level 1 and 2).

At each locus, low quality transcript models were removed, and the data were collapsed and consolidated into a final gene model plus its associated non-redundant transcript set. When collapsing the data, priority was given to models derived from transcriptomic data, cDNA sequences and manually annotated sequences. For each putative

transcript, the coverage of the longest open reading frame was assessed in relation to known vertebrate proteins, to help differentiate between true isoforms and fragments. In loci where the transcriptomic data were fragmented or missing, homology data was used to gap fill if a more complete cross-species alignment was available, with preference given to longer transcripts that had strong intron support from the short-read data.

Gene models were classified, based on the alignment quality of their supporting evidence, into three main types: protein-coding, pseudogene, and long non-coding RNA. Models with hits to known proteins, and few structural abnormalities (i.e., they had canonical splice sites, introns passing a minimum size threshold, low level of repeat coverage) were classified as protein-coding. Models with hits to known protein, but having multiple issues in their underlying structure, were classified as pseudogenes. Single-exon models with a corresponding multi-exon copy elsewhere in the genome were classified as processed pseudogenes.

If a model failed to meet the criteria of any of the previously described categories, did not overlap a protein-coding gene, and had been constructed from transcriptomic data then it was considered as a potential lncRNA. Potential lncRNAs were filtered to remove transcripts that did not have at least two valid splice sites or cover 1000bp (to remove transcriptional noise).

A separate pipeline was run to annotate small non-coding genes. miRNAs were annotated via a BLAST [101] of miRbase [102] against the genome, before passing the results into RNAfold. [103] Poor quality and repeat-ridden alignments were discarded. Other types of small non-coding genes were annotated by scanning Rfam [104] against the genome and passing the results into Infernal. [105]

The annotation for the rat assembly was made available as part of Ensembl release 105.

RefSeq Annotation. Annotation of the mRatBN7.2 assembly was generated for NCBI's RefSeq dataset [100] using NCBI's Eukaryotic Genome Annotation Pipeline [106]. The annotation, referred to as NCBI *Rattus norvegicus* Annotation Release 108, includes gene models from curated and computational sources for protein-coding and non-coding genes and pseudogenes, and is available from NCBI's genome FTP site and web resources.

Most protein-coding genes and some non-coding genes are represented by at least one known RefSeq transcript, labeled by the method “BestRefSeq” and assigned a transcript accession starting with NM_ or NR_, and corresponding RefSeq proteins designated with NP_ accessions. These are predominantly based on rat mRNAs subject to manual and automated curation by the RefSeq team for over 20 years, including automated quality analyses and comparisons to the Rnor_6.0 and mRatBN7.2 assemblies to refine the annotations. Nearly 80% of the protein-coding genes in AR108 include at least one NM_ RefSeq transcript, of which 33% have been fully reviewed by RefSeq curators.

Additional gene, transcript, and protein models were predicted using NCBI’s Gnomon algorithm using alignments of transcripts, proteins, and RNA-seq data as evidence. The evidence datasets used for Release 108 are described at https://www.ncbi.nlm.nih.gov/genome/annotation_euk/Rattus_norvegicus/108/, and included alignments of available rat mRNAs and ESTs, 10.7 billion RNA-seq reads from 303 SRA runs from a wide range of samples, 1 million Oxford Nanopore or PacBio transcript reads from 5 SRA runs, and known RefSeq proteins from human, mouse, and rat. BestRefSeq and Gnomon models were combined to generate the final annotation, compared to the previous Release 106 annotation of Rnor_6.0 to retain GeneID, transcript, and protein accessions for equivalent annotations, and compared to the RefSeq annotation of human GRCh38 to identify orthologous genes. Gene nomenclature was based on data from RGD, curated names, and human orthologs.

References

1. Richter, C.P. (1954). The effects of domestication and selection on the behavior of the Norway rat. J. Natl. Cancer Inst. *15*, 727–738.

2. Hulme-Beaman, A., Orton, D., and Cucchi, T. (2021). The origins of the domesticate brown rat (Rattus norvegicus) and its pathways to domestication. Anim Front *11*, 78–86.

3. Modlinska, K., and Pisula, W. (2020). The Norway rat, from an obnoxious pest to a laboratory pet. Elife *9*. 10.7554/eLife.50651.

4. Parker, C.C., Chen, H., Flagel, S.B., Geurts, A.M., Richards, J.B., Robinson, T.E., Solberg Woods, L.C., and Palmer, A.A. (2013). Rats are the smart choice: Rationale for a renewed focus on rats in behavioral genetics. Neuropharmacology *76 Pt B*, 250–258.

5. Smith, J.R., Hayman, G.T., Wang, S.-J., Laulederkind, S.J.F., Hoffman, M.J., Kaldunski, M.L., Tutaj, M., Thota, J., Nalabolu, H.S., Ellanki, S.L.R., et al. (2020). The Year of the Rat: The Rat Genome Database at 20: a multi-species knowledgebase and analysis platform. Nucleic Acids Res. *48*, D731–D742.

6. RRRC (2021). Rat Resource & Research Center - Rat Models. https://www.rrrc.us/.

7. Pravenec, M., Klír, P., Kren, V., Zicha, J., and Kunes, J. (1989). An analysis of spontaneous hypertension in spontaneously hypertensive rats by means of new recombinant inbred strains. J. Hypertens. *7*, 217–221.

8. Voigt, B., Kuramoto, T., Mashimo, T., Tsurumi, T., Sasaki, Y., Hokao, R., and Serikawa, T. (2008). Evaluation of LEXF/FXLE rat recombinant inbred strains for genetic dissection of complex traits. Physiol. Genomics *32*, 335–342.

9. Tabakoff, B., Smith, H., Vanderlinden, L.A., Hoffman, P.L., and Saba, L.M. (2019). Rat Genomics book. Methods Mol. Biol. *2018*, 213–231.

10. Hansen, C., and Spuhler, K. (1984). Development of the National Institutes of Health genetically heterogeneous rat stock. Alcohol. Clin. Exp. Res. *8*, 477–479.

11. Baud, A., Hermsen, R., Guryev, V., Stridh, P., Graham, D., McBride, M.W., Foroud, T., Calderari, S., Diez, M., Ockinger, J., et al. (2013). Combined sequence-based and genetic mapping analysis of complex traits in outbred rats. Nat. Genet. *45*, 767–775.

12. Woods, L.C.S., and Mott, R. (2017). Heterogeneous Stock Populations for Analysis of Complex Traits. Methods Mol. Biol. *1488*, 31–44.

13. Solberg Woods, L.C., and Palmer, A.A. (2019). Using Heterogeneous Stocks for Fine-Mapping Genetically Complex Traits. Methods Mol. Biol. *2018*, 233–247.

14. Chitre, A.S., Polesskaya, O., Holl, K., Gao, J., Cheng, R., Bimschleger, H., Garcia Martinez, A., George, T., Gileta, A.F., Han, W., et al. (2020). Genome-Wide Association Study in

3,173 Outbred Rats Identifies Multiple Loci for Body Weight, Adiposity, and Fasting Glucose. Obesity *28*, 1964–1973.

15. Gunturkun, M.H., Wang, T., Chitre, A.S., Garcia Martinez, A., Holl, K., St Pierre, C., Bimschleger, H., Gao, J., Cheng, R., Polesskaya, O., et al. (2022). Genome-Wide Association Study on Three Behaviors Tested in an Open Field in Heterogeneous Stock Rats Identifies Multiple Loci Implicated in Psychiatric Disorders. Front. Psychiatry *13*, 790566.

16. Kaldunski, M.L., Smith, J.R., Hayman, G.T., Brodie, K., De Pons, J.L., Demos, W.M., Gibson, A.C., Hill, M.L., Hoffman, M.J., Lamers, L., et al. (2022). The Rat Genome Database (RGD) facilitates genomic and phenotypic data integration across multiple species for biomedical research. Mamm. Genome *33*, 66–80.

17. Gibbs, R.A., Weinstock, G.M., Metzker, M.L., Muzny, D.M., Sodergren, E.J., Scherer, S., Scott, G., Steffen, D., Worley, K.C., Burch, P.E., et al. (2004). Genome sequence of the Brown Norway rat yields insights into mammalian evolution. Nature *428*, 493–521.

18. Worley, K.C., Weinstock, G.M., and Gibbs, R.A. (2008). Rats in the genomic era. Physiol. Genomics *32*, 273–282.

19. Twigger, S.N., Pruitt, K.D., Fernández-Suárez, X.M., Karolchik, D., Worley, K.C., Maglott, D.R., Brown, G., Weinstock, G., Gibbs, R.A., Kent, J., et al. (2008). What everybody should know about the rat genome and its online resources. Nat. Genet. *40*, 523–527.

20. van Heesch, S., Kloosterman, W.P., Lansu, N., Ruzius, F.-P., Levandowsky, E., Lee, C.C., Zhou, S., Goldstein, S., Schwartz, D.C., Harkins, T.T., et al. (2013). Improving mammalian genome scaffolding using large insert mate-pair next-generation sequencing. BMC Genomics *14*, 257.

21. Tutaj, M., Smith, J.R., and Bolton, E.R. (2019). Rat Genome Assemblies, Annotation, and Variant Repository. In Rat Genomics, G. T. Hayman, J. R. Smith, M. R. Dwinell, and M. Shimoyama, eds. (Springer New York), pp. 43–70.

22. Ramdas, S., Ozel, A.B., Treutelaar, M.K., Holl, K., Mandel, M., Woods, L.C.S., and Li, J.Z. (2019). Extended regions of suspected mis-assembly in the rat reference genome. Sci Data *6*, 39.

23. Howe, K., Dwinell, M., Shimoyama, M., Corton, C., Betteridge, E., Dove, A., Quail, M.A., Smith, M., Saba, L., Williams, R.W., et al. (2021). The genome sequence of the Norway rat, *Rattus norvegicus* Berkenhout 1769. Wellcome Open Res. *6*, 118.

24. Howe, K., Chow, W., Collins, J., Pelan, S., Pointon, D.-L., Sims, Y., Torrance, J., Tracey, A., and Wood, J. (2021). Significantly improving the quality of genome assemblies through curation. Gigascience *10*. 10.1093/gigascience/giaa153.

25. Poplin, R., Chang, P.-C., Alexander, D., Schwartz, S., Colthurst, T., Ku, A., Newburger, D., Dijamco, J., Nguyen, N., Afshar, P.T., et al. (2018). A universal SNP and small-indel variant caller using deep neural networks. Nat. Biotechnol. 10.1038/nbt.4235.

26. Yun, T., Li, H., Chang, P.-C., Lin, M.F., Carroll, A., and McLean, C.Y. (2020). Accurate,

scalable cohort variant calls using DeepVariant and GLnexus. Cold Spring Harbor Laboratory, 2020.02.10.942086. 10.1101/2020.02.10.942086.

27. Manni, M., Berkeley, M.R., Seppey, M., Simão, F.A., and Zdobnov, E.M. (2021). BUSCO Update: Novel and Streamlined Workflows along with Broader and Deeper Phylogenetic Coverage for Scoring of Eukaryotic, Prokaryotic, and Viral Genomes. Mol. Biol. Evol. *38*, 4647–4654.

28. Zhou, X., Li, R., Michal, J.J., Wu, X.-L., Liu, Z., Zhao, H., Xia, Y., Du, W., Wildung, M.R., Pouchnik, D.J., et al. (2016). Accurate Profiling of Gene Expression and Alternative Polyadenylation with Whole Transcriptome Termini Site Sequencing (WTTS-Seq). Genetics *203*, 683–697.

29. Munro, D., Wang, T., Chitre, A.S., Polesskaya, O., Ehsan, N., Gao, J., Gusev, A., Woods, L.C.S., Saba, L.M., Chen, H., et al. (2022). The regulatory landscape of multiple brain regions in outbred heterogeneous stock rats. Nucleic Acids Res. 10.1093/nar/gkac912.

30. Canzian, F. (1997). Phylogenetics of the laboratory rat Rattus norvegicus. Genome Res. *7*, 262–267.

31. Thomas, M.A., Chen, C.-F., Jensen-Seaman, M.I., Tonellato, P.J., and Twigger, S.N. (2003). Phylogenetics of rat inbred strains. Mamm. Genome *14*, 61–64.

32. Mashimo, T., Voigt, B., Tsurumi, T., Naoi, K., Nakanishi, S., Yamasaki, K.-I., Kuramoto, T., and Serikawa, T. (2006). A set of highly informative rat simple sequence length polymorphism (SSLP) markers and genetically defined rat strains. BMC Genet. *7*, 19.

33. Atanur, S.S., Diaz, A.G., Maratou, K., Sarkis, A., Rotival, M., Game, L., Tschannen, M.R., Kaisaki, P.J., Otto, G.W., Ma, M.C.J., et al. (2013). Genome sequencing reveals loci under artificial selection that underlie disease phenotypes in the laboratory rat. Cell *154*, 691–703.

34. Martín-Gálvez, D., Dunoyer de Segonzac, D., Ma, M.C.J., Kwitek, A.E., Thybert, D., and Flicek, P. (2017). Genome variation and conserved regulation identify genomic regions responsible for strain specific phenotypes in rat. BMC Genomics *18*, 986.

35. Ma, M.C.J., Atanur, S.S., Aitman, T.J., and Kwitek, A.E. (2014). Genomic structure of nucleotide diversity among Lyon rat models of metabolic syndrome. BMC Genomics *15*, 197.

36. Buniello, A., MacArthur, J.A.L., Cerezo, M., Harris, L.W., Hayhurst, J., Malangone, C., McMahon, A., Morales, J., Mountjoy, E., Sollis, E., et al. (2019). The NHGRI-EBI GWAS Catalog of published genome-wide association studies, targeted arrays and summary statistics 2019. Nucleic Acids Res. *47*, D1005–D1012.

37. Walker, B.J., Abeel, T., Shea, T., Priest, M., Abouelliel, A., Sakthikumar, S., Cuomo, C.A., Zeng, Q., Wortman, J., Young, S.K., et al. (2014). Pilon: An Integrated Tool for Comprehensive Microbial Variant Detection and Genome Assembly Improvement. PLoS One *9*, e112963.

38. Mikheenko, A., Prjibelski, A., Saveliev, V., Antipov, D., and Gurevich, A. (2018). Versatile genome assembly evaluation with QUAST-LG. Bioinformatics *34*, i142–i150.

39. Rhie, A., Walenz, B.P., Koren, S., and Phillippy, A.M. (2020). Merqury: reference-free quality, completeness, and phasing assessment for genome assemblies. Genome Biol. *21*, 245.

40. Koren, S., Phillippy, A.M., Simpson, J.T., Loman, N.J., and Loose, M. (2019). Reply to "Errors in long-read assemblies can critically affect protein prediction." Nat. Biotechnol. *37*, 127–128.

41. Watson, M., and Warr, A. (2019). Errors in long-read assemblies can critically affect protein prediction. Nat. Biotechnol. *37*, 124–126.

42. Sacristán-Horcajada, E., González-de la Fuente, S., Peiró-Pastor, R., Carrasco-Ramiro, F., Amils, R., Requena, J.M., Berenguer, J., and Aguado, B. (2021). ARAMIS: From systematic errors of NGS long reads to accurate assemblies. Brief. Bioinform. *22*. 10.1093/bib/bbab170.

43. Rhie, A., McCarthy, S.A., Fedrigo, O., Damas, J., Formenti, G., Koren, S., Uliano-Silva, M., Chow, W., Fungtammasan, A., Kim, J., et al. (2021). Towards complete and error-free genome assemblies of all vertebrate species. Nature *592*, 737–746.

44. Chin, C.-S., Peluso, P., Sedlazeck, F.J., Nattestad, M., Concepcion, G.T., Clum, A., Dunn, C., O'Malley, R., Figueroa-Balderas, R., Morales-Cruz, A., et al. (2016). Phased diploid genome assembly with single-molecule real-time sequencing. Nat. Methods *13*, 1050–1054.

45. de Jong, T.V., Chen, H., Brashear, W.A., Kochan, K.J., Hillhouse, A.E., Zhu, Y., Dhande, I.S., Hudson, E.A., Sumlut, M.H., Smith, M.L., et al. (2022). mRatBN7.2: familiar and unfamiliar features of a new rat genome reference assembly. Physiol. Genomics *54*, 251–260.

46. Nurk, S., Koren, S., Rhie, A., Rautiainen, M., Bzikadze, A.V., Mikheenko, A., Vollger, M.R., Altemose, N., Uralsky, L., Gershman, A., et al. (2022). The complete sequence of a human genome. Science *376*, 44–53.

47. Hermsen, R., de Ligt, J., Spee, W., Blokzijl, F., Schäfer, S., Adami, E., Boymans, S., Flink, S., van Boxtel, R., van der Weide, R.H., et al. (2015). Genomic landscape of rat strain and substrain variation. BMC Genomics *16*, 357.

48. Supernat, A., Vidarsson, O.V., Steen, V.M., and Stokowy, T. (2018). Comparison of three variant callers for human whole genome sequencing. Sci. Rep. *8*, 17851.

49. Ashbrook, D.G., Arends, D., Prins, P., Mulligan, M.K., Roy, S., Williams, E.G., Lutz, C.M., Valenzuela, A., Bohl, C.J., Ingels, J.F., et al. (2021). A platform for experimental precision medicine: The extended BXD mouse family. Cell Syst *12*, 235–247.e9.

50. Ashbrook, D.G., Sasani, T., Maksimov, M., Gunturkun, M.H., Ma, N., Villani, F., Ren, Y., Rothschild, D., Chen, H., Lu, L., et al. (2022). Private and sub-family specific mutations of founder haplotypes in the BXD family reveal phenotypic consequences relevant to health and disease. bioRxiv, 2022.04.21.489063. 10.1101/2022.04.21.489063.

51. Pattee, J., Vanderlinden, L.A., Mahaffey, S., Hoffman, P., Tabakoff, B., and Saba, L.M.

(2022). Evaluation and characterization of expression quantitative trait analysis methods in the Hybrid Rat Diversity Panel. Front. Genet. *13*, 947423.

52. Senko, A.N., Overall, R.W., Silhavy, J., Mlejnek, P., Malínská, H., Hüttl, M., Marková, I., Fabel, K.S., Lu, L., Stuchlik, A., et al. (2022). Systems genetics in the rat HXB/BXH family identifies Tti2 as a pleiotropic quantitative trait gene for adult hippocampal neurogenesis and serum glucose. PLoS Genet. *18*, e1009638.

53. Bryant, C.D., Smith, D.J., Kantak, K.M., Nowak, T.S., Jr, Williams, R.W., Damaj, M.I., Redei, E.E., Chen, H., and Mulligan, M.K. (2020). Facilitating Complex Trait Analysis via Reduced Complexity Crosses. Trends Genet. *36*, 549–562.

54. Witte, F., Ruiz-Orera, J., Mattioli, C.C., Blachut, S., Adami, E., Schulz, J.F., Schneider-Lunitz, V., Hummel, O., Patone, G., Mücke, M.B., et al. (2021). A trans locus causes a ribosomopathy in hypertrophic hearts that affects mRNA translation in a protein length-dependent fashion. Genome Biol. *22*, 191.

55. Pravenec, M., Kožich, V., Krijt, J., Sokolová, J., Zídek, V., Landa, V., Mlejnek, P., Šilhavý, J., Šimáková, M., Škop, V., et al. (2016). Genetic Variation in Renal Expression of Folate Receptor 1 (Folr1) Gene Predisposes Spontaneously Hypertensive Rats to Metabolic Syndrome. Hypertension *67*, 335–341.

56. Pravenec, M., Churchill, P.C., Churchill, M.C., Viklicky, O., Kazdova, L., Aitman, T.J., Petretto, E., Hubner, N., Wallace, C.A., Zimdahl, H., et al. (2008). Identification of renal Cd36 as a determinant of blood pressure and risk for hypertension. Nat. Genet. *40*, 952–954.

57. Heinig, M., Petretto, E., Wallace, C., Bottolo, L., Rotival, M., Lu, H., Li, Y., Sarwar, R., Langley, S.R., Bauerfeind, A., et al. (2010). A trans-acting locus regulates an anti-viral expression network and type 1 diabetes risk. Nature *467*, 460–464.

58. Lu, L.M., Shisa, H., Tanuma, J., and Hiai, H. (1999). Propylnitrosourea-induced T-lymphomas in LEXF RI strains of rats: genetic analysis. Br. J. Cancer *80*, 855–861.

59. Hubner, N., Wallace, C.A., Zimdahl, H., Petretto, E., Schulz, H., Maciver, F., Mueller, M., Hummel, O., Monti, J., Zidek, V., et al. (2005). Integrated transcriptional profiling and linkage analysis for identification of genes underlying disease. Nat. Genet. *37*, 243–253.

60. Holl, K., He, H., Wedemeyer, M., Clopton, L., Wert, S., Meckes, J.K., Cheng, R., Kastner, A., Palmer, A.A., Redei, E.E., et al. (2018). Heterogeneous stock rats: a model to study the genetics of despair-like behavior in adolescence. Genes Brain Behav. *17*, 139–148.

61. Keele, G.R., Prokop, J.W., He, H., Holl, K., Littrell, J., Deal, A., Francic, S., Cui, L., Gatti, D.M., Broman, K.W., et al. (2018). Genetic Fine-Mapping and Identification of Candidate Genes and Variants for Adiposity Traits in Outbred Rats. Obesity *26*, 213–222.

62. Solberg Woods, L.C., Holl, K.L., Oreper, D., Xie, Y., Tsaih, S.-W., and Valdar, W. (2012). Fine-mapping diabetes-related traits, including insulin resistance, in heterogeneous stock rats. Physiol. Genomics *44*, 1013–1026.

63. Lemen, P.M., Hatoum, A.S., Dickson, P.E., Mittleman, G., Agrawal, A., Reiner, B.C.,

Berrettini, W., Ashbrook, D., Gunturkun, H., Mulligan, M.K., et al. (2022). Opiate responses are controlled by interactions of Oprm1 and Fgf12 loci in the murine BXD family: Correspondence to human GWAS finding. bioRxiv, 2022.03.11.483993. 10.1101/2022.03.11.483993.

64. Lusis, A.J., Seldin, M.M., Allayee, H., Bennett, B.J., Civelek, M., Davis, R.C., Eskin, E., Farber, C.R., Hui, S., Mehrabian, M., et al. (2016). The Hybrid Mouse Diversity Panel: a resource for systems genetics analyses of metabolic and cardiovascular traits. J. Lipid Res. *57*, 925–942.

65. Ulusoy, S., Ozkan, G., Alkanat, M., Mungan, S., Yuluğ, E., and Orem, A. (2013). Perspective on rhabdomyolysis-induced acute kidney injury and new treatment options. Am. J. Nephrol. *38*, 368–378.

66. Kang, K., Nan, C., Fei, D., Meng, X., Liu, W., Zhang, W., Jiang, L., Zhao, M., Pan, S., and Zhao, M. (2013). Heme oxygenase 1 modulates thrombomodulin and endothelial protein C receptor levels to attenuate septic kidney injury. Shock *40*, 136–143.

67. Yuan, G., Deng, J., Wang, T., Zhao, C., Xu, X., Wang, P., Voltz, J.W., Edin, M.L., Xiao, X., Chao, L., et al. (2007). Tissue kallikrein reverses insulin resistance and attenuates nephropathy in diabetic rats by activation of phosphatidylinositol 3-kinase/protein kinase B and adenosine 5'-monophosphate-activated protein kinase signaling pathways. Endocrinology *148*, 2016–2026.

68. Osipova, E., Barsacchi, R., Brown, T., Sadanandan, K., Gaede, A.H., Monte, A., Jarrells, J., Moebius, C., Pippel, M., Altshuler, D.L., et al. (2023). Loss of a gluconeogenic muscle enzyme contributed to adaptive metabolic traits in hummingbirds. Science *379*, 185–190.

69. Obeidat, M. 'en, Zhou, G., Li, X., Hansel, N.N., Rafaels, N., Mathias, R., Ruczinski, I., Beaty, T.H., Barnes, K.C., Paré, P.D., et al. (2018). The genetics of smoking in individuals with chronic obstructive pulmonary disease. Respir. Res. *19*, 59.

70. Chen, N.-C., Solomon, B., Mun, T., Iyer, S., and Langmead, B. (2021). Reference flow: reducing reference bias using multiple population genomes. Genome Biol. *22*, 8.

71. Munger, S.C., Raghupathy, N., Choi, K., Simons, A.K., Gatti, D.M., Hinerfeld, D.A., Svenson, K.L., Keller, M.P., Attie, A.D., Hibbs, M.A., et al. (2014). RNA-Seq alignment to individualized genomes improves transcript abundance estimates in multiparent populations. Genetics *198*, 59–73.

72. Eizenga, J.M., Novak, A.M., Sibbesen, J.A., Heumos, S., Ghaffaari, A., Hickey, G., Chang, X., Seaman, J.D., Rounthwaite, R., Ebler, J., et al. (2020). Pangenome Graphs. Annu. Rev. Genomics Hum. Genet. *21*, 139–162.

73. Kalbfleisch, T.S., Hussien AbouEl Ela, N.A., Li, K., Brashear, W.A., Kochan, K.J., Hillhouse, A.E., Zhu, Y., Dhande, I.S., Kline, E.J., Hudson, E.A., et al. (2023). The Assembled Genome of the Stroke-Prone Spontaneously Hypertensive Rat. Hypertension *80*, 138–146.

74. Rastas, P. (2020). Lep-Anchor: automated construction of linkage map anchored haploid genomes. Bioinformatics *36*, 2359–2364.

75. Kivikoski, M., Rastas, P., Löytynoja, A., and Merilä, J. (2021). Automated improvement of stickleback reference genome assemblies with Lep-Anchor software. Mol. Ecol. Resour. *21*, 2166–2176.

76. ENCODE Project Consortium (2012). An integrated encyclopedia of DNA elements in the human genome. Nature *489*, 57–74.

77. Kalikar, S., Jain, C., Vasimuddin, and Misra, S. (2022). Accelerating minimap2 for long-read sequencing applications on modern CPUs. Nature Computational Science *2*, 78–83.

78. Li, H., and Durbin, R. (2010). Fast and accurate long-read alignment with Burrows-Wheeler transform. Bioinformatics *26*, 589–595.

79. Poplin, R., Ruano-Rubio, V., DePristo, M.A., Fennell, T.J., Carneiro, M.O., Van der Auwera, G.A., Kling, D.E., Gauthier, L.D., Levy-Moonshine, A., Roazen, D., et al. (2018). Scaling accurate genetic variant discovery to tens of thousands of samples. bioRxiv, 201178. 10.1101/201178.

80. Li, H. (2018). Minimap2: pairwise alignment for nucleotide sequences. Bioinformatics *34*, 3094–3100.

81. Jeffares, D.C., Jolly, C., Hoti, M., Speed, D., Shaw, L., Rallis, C., Balloux, F., Dessimoz, C., Bähler, J., and Sedlazeck, F.J. (2017). Transient structural variations have strong effects on quantitative traits and reproductive isolation in fission yeast. Nat. Commun. *8*, 14061.

82. Cingolani, P., Platts, A., Wang, L.L., Coon, M., Nguyen, T., Wang, L., Land, S.J., Lu, X., and Ruden, D.M. (2012). A program for annotating and predicting the effects of single nucleotide polymorphisms, SnpEff: SNPs in the genome of Drosophila melanogaster strain w1118; iso-2; iso-3. Fly *6*, 80–92.

83. Tarailo-Graovac, M., and Chen, N. (2009). Using RepeatMasker to identify repetitive elements in genomic sequences. Curr. Protoc. Bioinformatics *Chapter 4*, Unit 4.10.

84. Gunturkun, M.H., Flashner, E., Wang, T., Mulligan, M.K., Williams, R.W., Prins, P., and Chen, H. (2022). GeneCup: mining PubMed and GWAS catalog for gene–keyword relationships. G3 Genes|Genomes|Genetics *12*, jkac059.

85. Hinrichs, A.S., Karolchik, D., Baertsch, R., Barber, G.P., Bejerano, G., Clawson, H., Diekhans, M., Furey, T.S., Harte, R.A., Hsu, F., et al. (2006). The UCSC Genome Browser Database: update 2006. Nucleic Acids Res. *34*, D590–D598.

86. Gileta, A.F., Gao, J., Chitre, A.S., Bimschleger, H.V., St Pierre, C.L., Gopalakrishnan, S., and Palmer, A.A. (2020). Adapting Genotyping-by-Sequencing and Variant Calling for Heterogeneous Stock Rats. G3 *10*, 2195–2205.

87. Purcell, S., Neale, B., Todd-Brown, K., Thomas, L., Ferreira, M.A.R., Bender, D., Maller, J., Sklar, P., de Bakker, P.I.W., Daly, M.J., et al. (2007). PLINK: a tool set for whole-genome association and population-based linkage analyses. Am. J. Hum. Genet. *81*, 559–575.

88. Rastas, P. (2017). Lep-MAP3: robust linkage mapping even for low-coverage whole genome sequencing data. Bioinformatics *33*, 3726–3732.

89. Danecek, P., Bonfield, J.K., Liddle, J., Marshall, J., Ohan, V., Pollard, M.O., Whitwham, A., Keane, T., McCarthy, S.A., Davies, R.M., et al. (2021). Twelve years of SAMtools and BCFtools. Gigascience *10*. 10.1093/gigascience/giab008.

90. Tamura, K., Stecher, G., and Kumar, S. (2021). MEGA11: Molecular Evolutionary Genetics Analysis Version 11. Mol. Biol. Evol. *38*, 3022–3027.

91. Yu, G., Smith, D.K., Zhu, H., Guan, Y., and Lam, T.T.-Y. (2017). Ggtree : An r package for visualization and annotation of phylogenetic trees with their covariates and other associated data. Methods Ecol. Evol. *8*, 28–36.

92. Dobin, A., Davis, C.A., Schlesinger, F., Drenkow, J., Zaleski, C., Jha, S., Batut, P., Chaisson, M., and Gingeras, T.R. (2012). STAR: ultrafast universal RNA-seq aligner. Bioinformatics *29*, 15–21.

93. Duttke, S.H., Montilla-Perez, P., Chang, M.W., Li, H., Chen, H., Carrette, L.L.G., de Guglielmo, G., George, O., Palmer, A.A., Benner, C., et al. (2022). Glucocorticoid Receptor-Regulated Enhancers Play a Central Role in the Gene Regulatory Networks Underlying Drug Addiction. Front. Neurosci. *16*, 858427.

94. Duttke, S.H., Chang, M.W., Heinz, S., and Benner, C. (2019). Identification and dynamic quantification of regulatory elements using total RNA. Genome Res. *29*, 1836–1846.

95. Zhou, J.L., de Guglielmo, G., Ho, A.J., Kallupi, M., Li, H.-R., Chitre, A.S., Carrette, L.L.G., George, O., Palmer, A.A., McVicker, G., et al. (2022). Cocaine addiction-like behaviors are associated with long-term changes in gene regulation, energy metabolism, and GABAergic inhibition within the amygdala. bioRxiv, 2022.09.08.506493. 10.1101/2022.09.08.506493.

96. Delaneau, O., Ongen, H., Brown, A.A., Fort, A., Panousis, N.I., and Dermitzakis, E.T. (2017). A complete tool set for molecular QTL discovery and analysis. Nat. Commun. *8*, 15452.

97. Jeffs, B., Negrin, C.D., Graham, D., Clark, J.S., Anderson, N.H., Gauguier, D., and Dominiczak, A.F. (2000). Applicability of a “speed” congenic strategy to dissect blood pressure quantitative trait loci on rat chromosome 2. Hypertension *35*, 179–187.

98. Aken, B.L., Ayling, S., Barrell, D., Clarke, L., Curwen, V., Fairley, S., Fernandez Banet, J., Billis, K., García Girón, C., Hourlier, T., et al. (2016). The Ensembl gene annotation system. Database *2016*. 10.1093/database/baw093.

99. UniProt Consortium (2019). UniProt: a worldwide hub of protein knowledge. Nucleic Acids Res. *47*, D506–D515.

100. O’Leary, N.A., Wright, M.W., Brister, J.R., Ciufo, S., Haddad, D., McVeigh, R., Rajput, B., Robbertse, B., Smith-White, B., Ako-Adjei, D., et al. (2016). Reference sequence (RefSeq) database at NCBI: current status, taxonomic expansion, and functional annotation. Nucleic Acids Res. *44*, D733–D745.

101. Altschul, S.F., Gish, W., Miller, W., Myers, E.W., and Lipman, D.J. (1990). Basic local alignment search tool. J. Mol. Biol. *215*, 403–410.

102. Kozomara, A., Birgaoanu, M., and Griffiths-Jones, S. (2019). miRBase: from microRNA sequences to function. Nucleic Acids Res. *47*, D155–D162.

103. Gruber, A.R., Lorenz, R., Bernhart, S.H., Neuböck, R., and Hofacker, I.L. (2008). The Vienna RNA websuite. Nucleic Acids Res. *36*, W70–W74.

104. Kalvari, I., Argasinska, J., Quinones-Olvera, N., Nawrocki, E.P., Rivas, E., Eddy, S.R., Bateman, A., Finn, R.D., and Petrov, A.I. (2018). Rfam 13.0: shifting to a genome-centric resource for non-coding RNA families. Nucleic Acids Res. *46*, D335–D342.

105. Nawrocki, E.P., and Eddy, S.R. (2013). Infernal 1.1: 100-fold faster RNA homology searches. Bioinformatics *29*, 2933–2935.

106. McGarvey, K.M., Goldfarb, T., Cox, E., Farrell, C.M., Gupta, T., Joardar, V.S., Kodali, V.K., Murphy, M.R., O'Leary, N.A., Pujar, S., et al. (2015). Mouse genome annotation by the RefSeq project. Mamm. Genome *26*, 379–390.

A revamped rat reference genome improves the discovery of genetic diversity in laboratory rats

Figure and legends

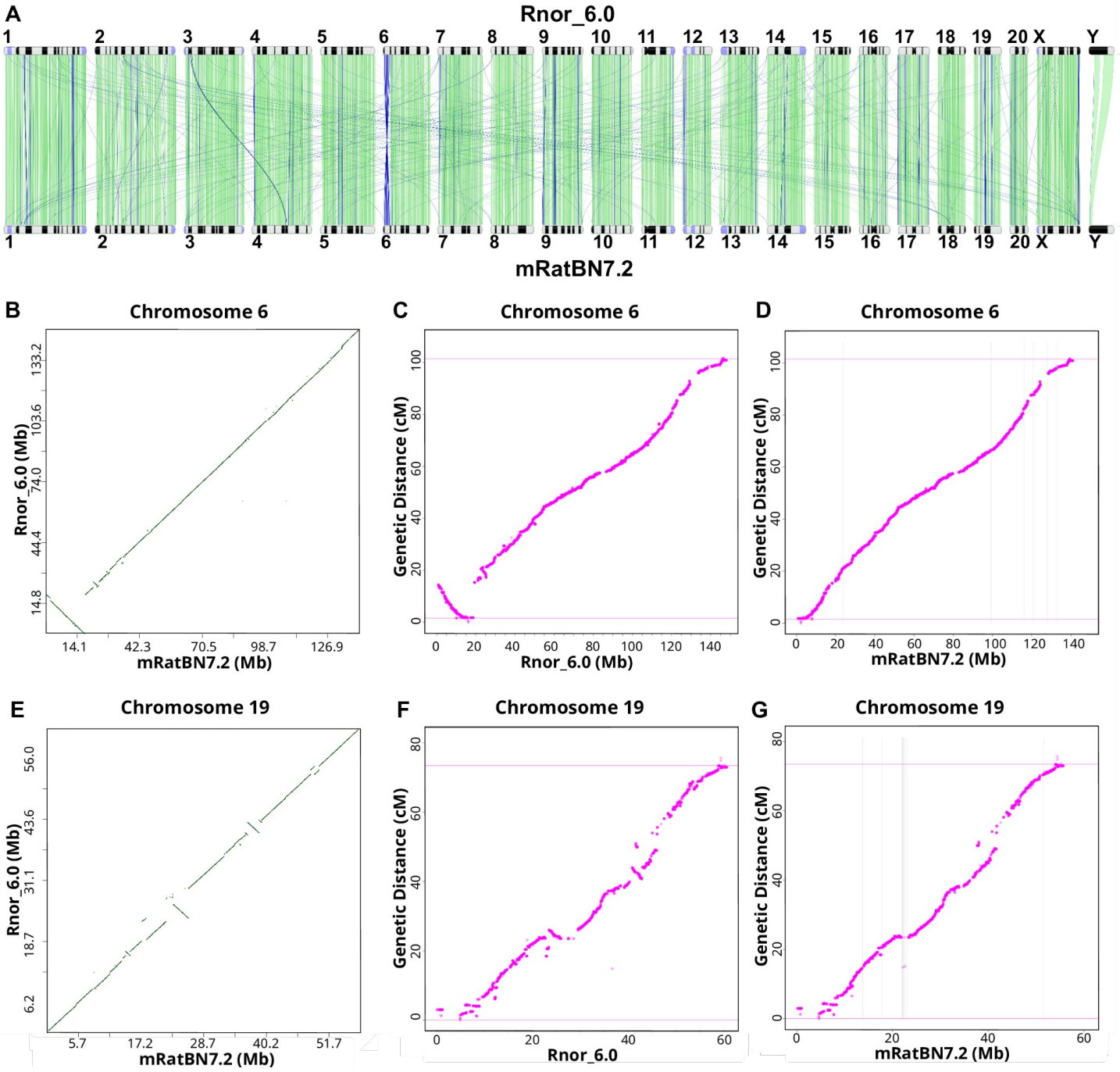

Figure 1. mRatBN7.2 corrects structural errors in Rnor_6.0

(A) Genome-wide comparison between Rnor_6.0 and mRatBN7.2 showed many structural differences between these two references, such as a large inversion at proximal Chr 6 and many translocations between chromosomes. Image generated using the NCBI Comparative Genome Viewer. Numbers indicate chromosomes. Green lines indicate sequences in the forward alignment. Blue lines indicate reverse alignment. **(B)** The large inversion on proximal Chr 6 is shown in a dot plot between Rnor_6.0 and mRatBN7.2. **(C)** A rat genetic map generated using 150,835 binned markers from 1,893 heterogeneous stock rats showed an inversion at proximal Chr 6 between genetic distance and and physical distance based on Rnor_6.0, indicating the inversion is caused by assembly errors in Rnor_6.0. **(D)** Marker order and genetic distance from the genetic map on Chr 6 are in agreement with physical distance based on mRatBN7.2, indication the misassembly is fixed. **(E-G)** Genetic map confirms many assembly errors on Chr 19 in Rnor_6.0 are fixed in mRatBN7.2.

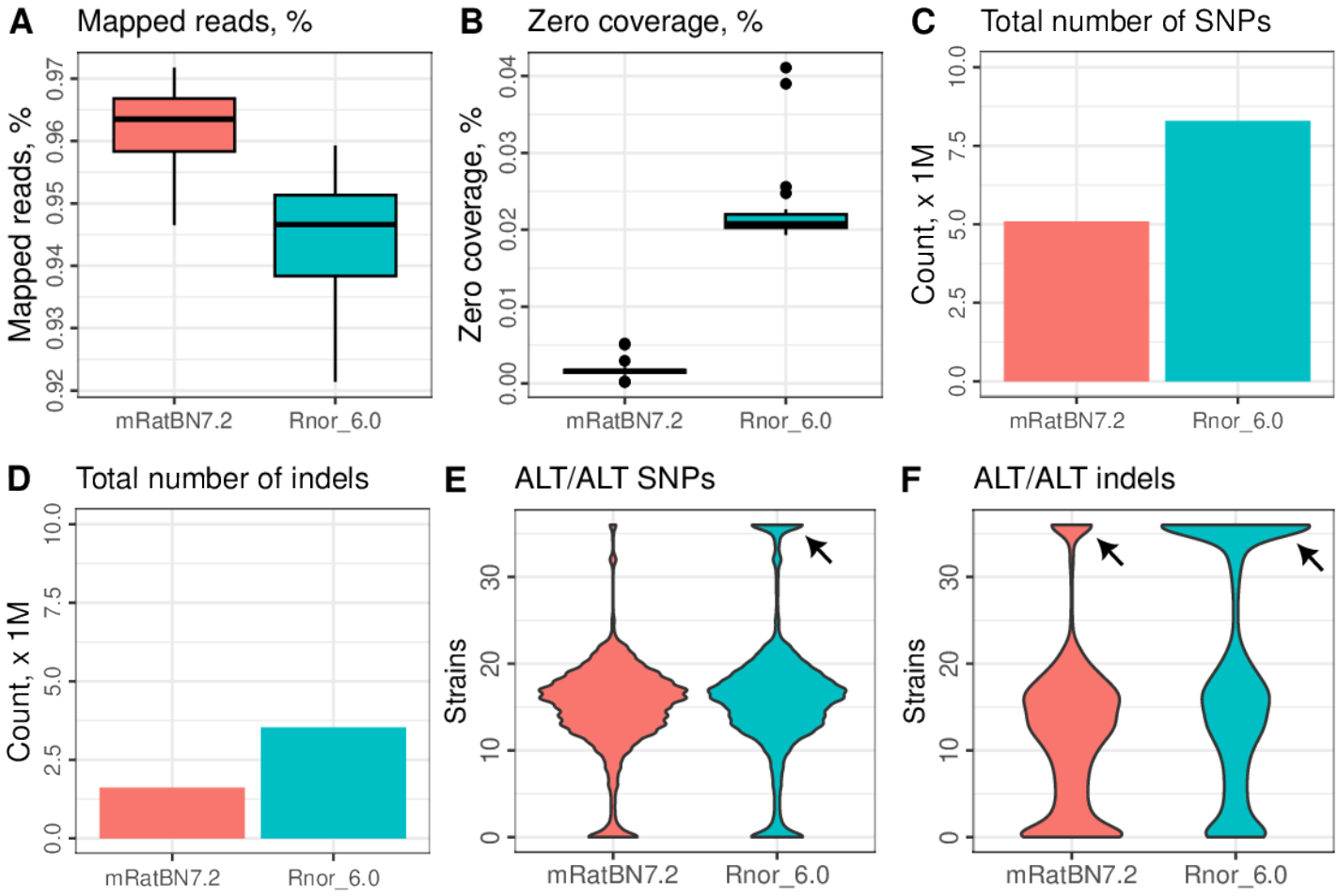

Figure 2. mRatBN7.2 improved mapping statistics of whole-genome sequencing data. Summary statistics from mapping 36 HXB/BXH WGS samples against Rnor_6.0 and mRatBN7.2 were compared. Using mRatBN7.2 increased percentage of reads mapped **(A)**, reduced percentage of regions on the reference genome with zero coverage **(B)**, total number of SNPs **(C)** and indels **(D)**. The presence of large number of SNPs **(E)** and indels **(F)** that are shared by all samples (arrows), including BN/NHsdMcwi, indicating they are base-level errors in the reference genome.

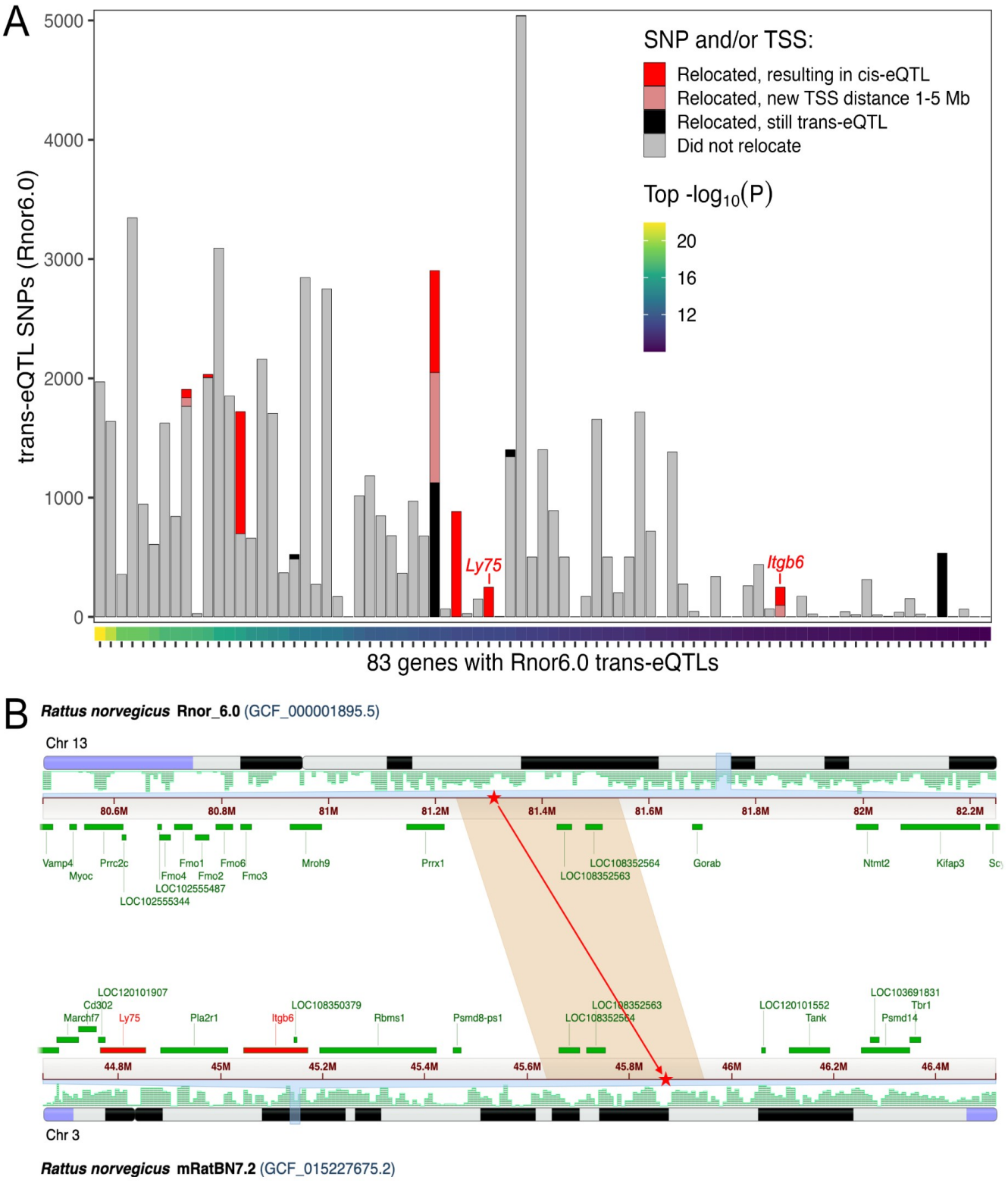

Figure 3. mRatBN7.2 improves eQTL analysis. Genome misassembly is associated with increased rates of calling spurious trans-eQTLs. We compared eQTL mapping using an existing RNA-seq data from nucleus accumbens core. **(A)** Each column represents a gene for which at least one trans-eQTL was found at P<1e-8 using Rnor_6.0. The color of bars indicate the number of trans-eQTL SNP-gene pairs in which the SNP and/or gene transcription start site (TSS) relocated to a different chromosome in mRatBN7.2, and whether the relocation would result in a reclassification to cis-eQTL (TSS distance <1 Mb) or ambiguous (TSS distance 1-5 Mb). **(B)** Genomic location of one relocated trans-eQTL SNP from A). The SNP is in a segment of Chr 13 in Rnor_6.0 that was relocated to Chr 3 in mRatBN7.2 (red stars), reclassifying the e-QTL from trans-eQTL to cis-eQTL for both Ly75 and Itgb6 genes (red bars).

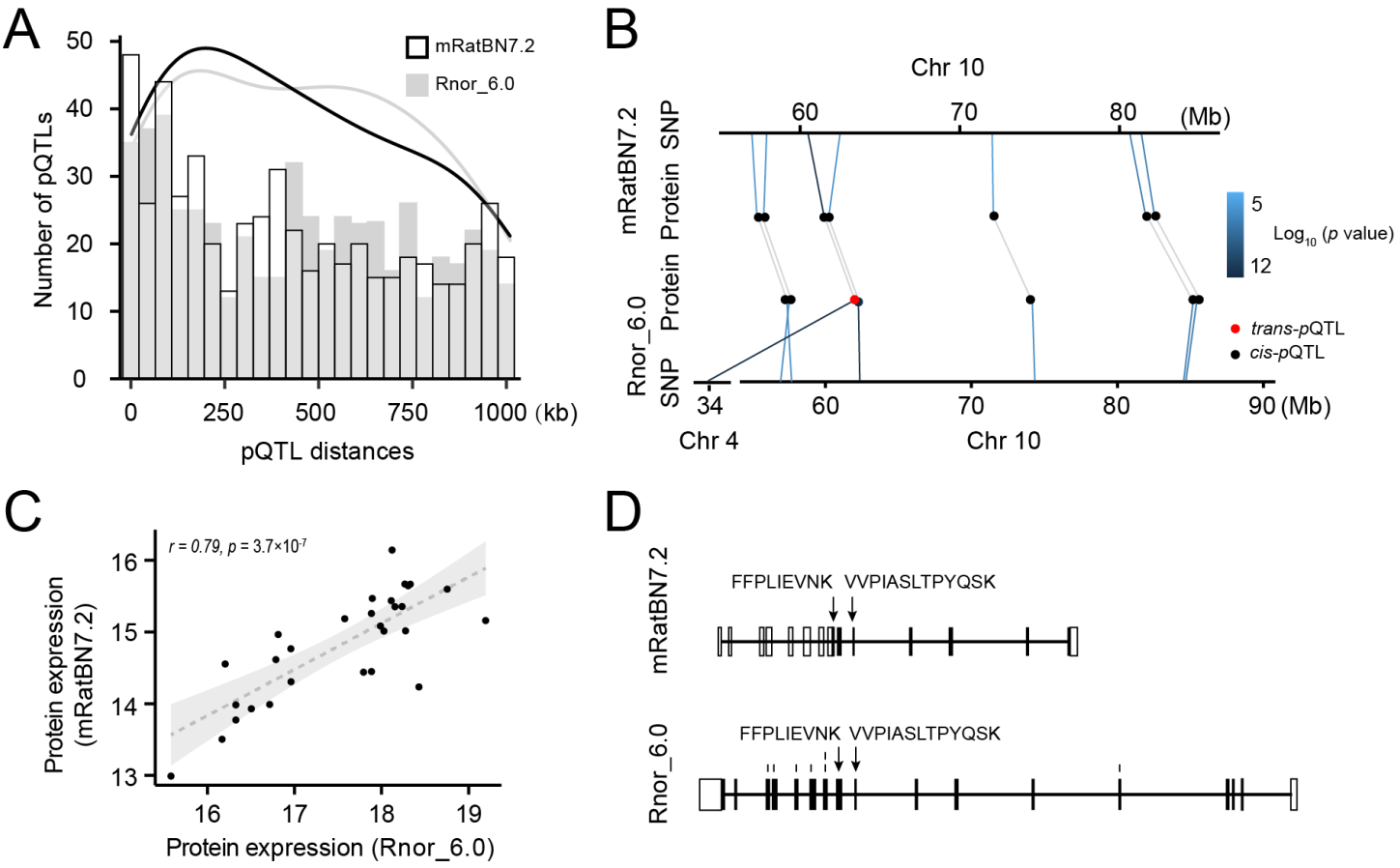

Figure 4. mRatBN7.2 improves the analysis of proteomic data. We compared protein identification and pQTL mapping using a brain proteome data. **(A)** Histogram showing the distance between cis-pQTLs and transcription starting site (TSS) of the corresponding proteins. The distances of pQTLs in mRatBN7.2 tend to be closer than those in Rnor_6.0. **(B)** An example of trans-pQTL in Rnor_6.0 was detected as a cis-pQTL in mRatBN7.2. C) Correlation of expression of the protein (the example in B) in Rnor_6.0 and mRatBN7.2. D) Different annotations of the exemplar gene in Rnor_6.0 and mRatBN7.2.

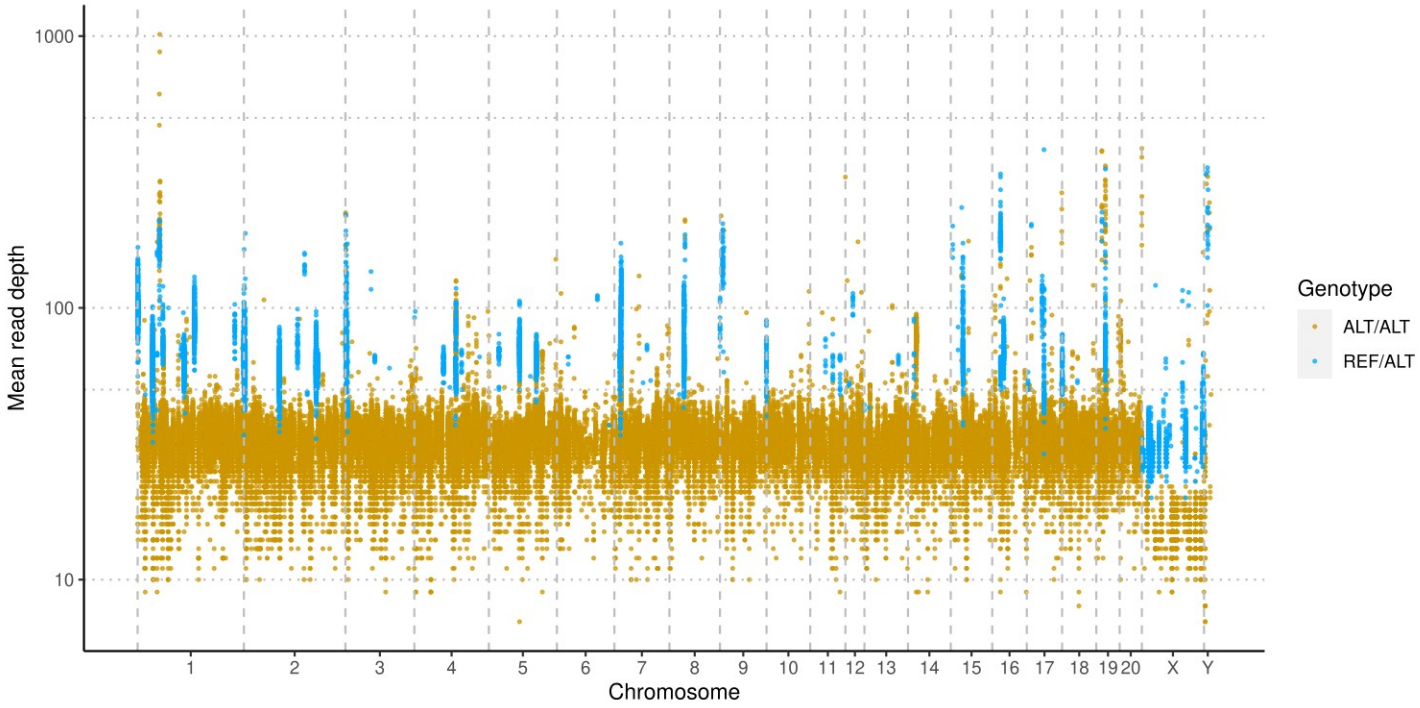

Figure 5. SNPs and indels indicate remaining errors in mRatBN7.2. Base-level errors are indicated by homozygous variants that are shared by the majority (i.e. more than 153 out of 163) of samples, including all seven BN/NHsdMcwi rats, one of them is part of the data used to assemble mRatBN7.2. Variants that are heterozygous for the majority of the samples are clustered in a few regions and have significantly higher read-depth. This suggests that they originated from collapsed repeats in mRatBN7.2.

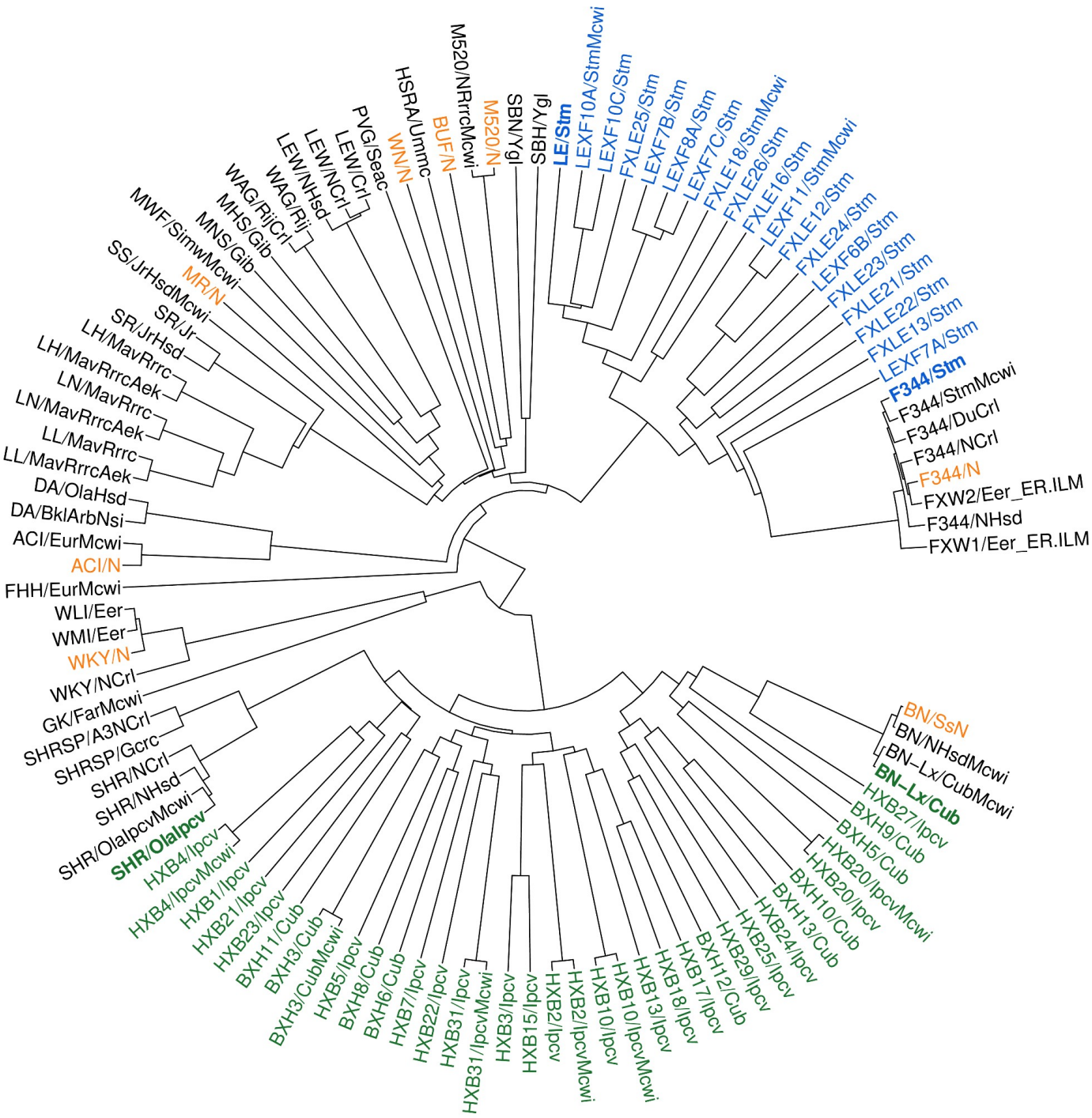

Figure 6. Phylogenetic relationship of 120 strain/substrains of laboratory rats. The phylogenetic tree was constructed using 11.6 million biallelic SNPs from 163 samples. Strains/substrains with duplicated samples were condensed. Strains highlighted with bold fonts are parental strains for RI panels. Green: HXB/BXH RI panel. Blue: FXLE/LEXF RI panel. Orange: progenitors of the HS outbred population.

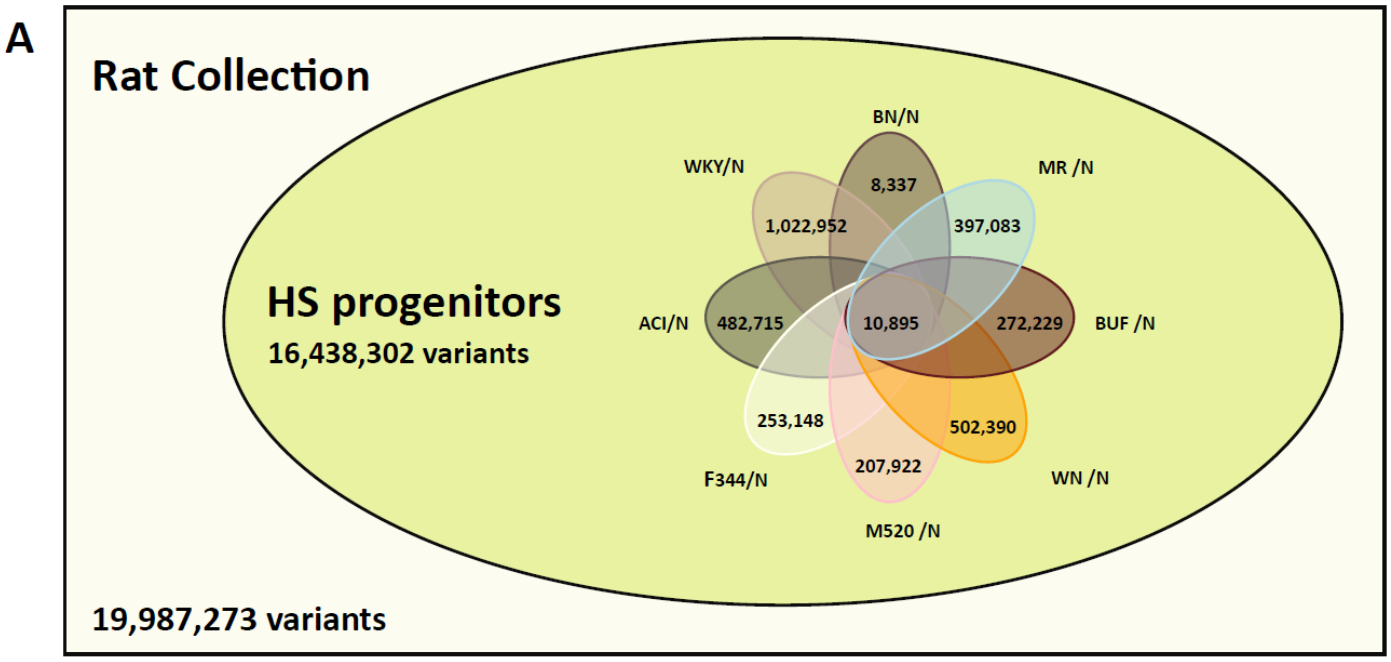

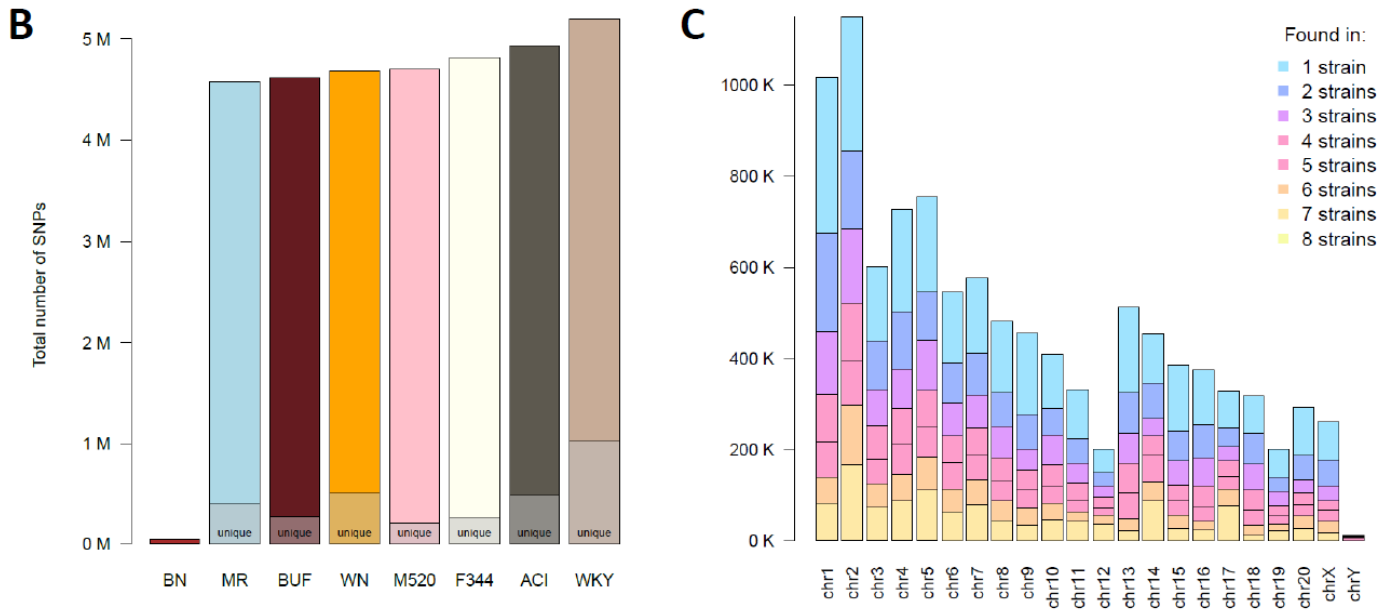

Figure 7. **Genetic diversity among progenitors of heterogeneous stock (HS) rats. (A)** The HS progenitors contain 16,438,302 variants (i.e., 82.2% of the variants in our collection of 120 strain/substrains) based on analysis using mRatBN7.2. Among these, 10,895 are shared by all eight progenitor strains. The number of variants that are unique to each specific founder is noted. **(B)** The total number of variants per strain, with the total number unique to each strain marked. **(C)** The number of variants shared across N strains, shown per chromosome.

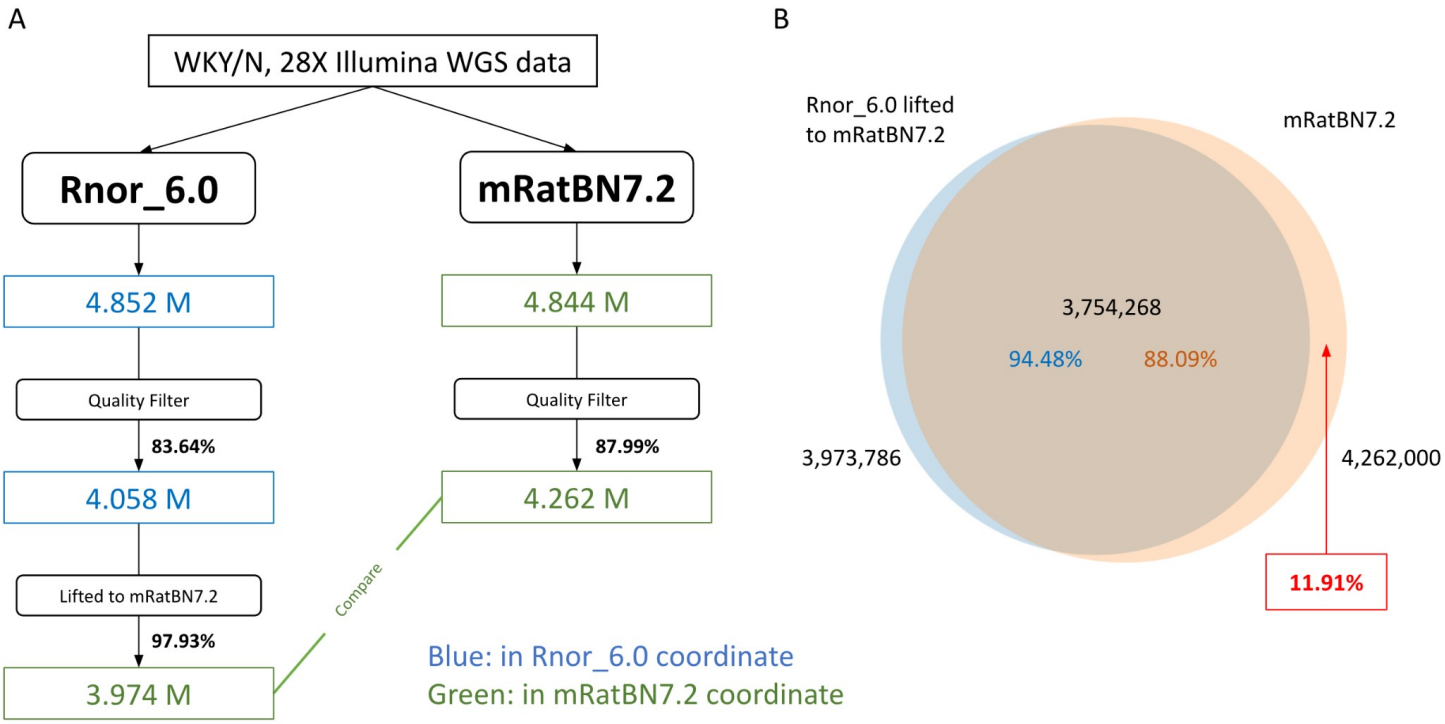

Figure 8. Using WGS data to assess the quality of the Liftover. LiftOver is a tool often used to translate genomic coordinates between versions of reference genomes. We evaluated the effectiveness of LiftOver from Rnor_6.0 to mRatBN7.2. **(A)** Overview of the workflow using a real WGS sample from a WKY rat. A higher portion of variants passed the quality filter for mRatBN7.2. Among them, 97.93% of the variants were liftable from Rnor_6.0 to mRatBN7.2. **(B)** The overlap between variants lifted from Rnor_6.0 and variants obtained by direct mapping sequence data to mRatBN7.2. Approximately 11.9% of the variants that found from direct mapping were missing from the liverover.